

ASPECTS OF A SEISMIC STUDY OF THE

MITR--

by

GEORGE C. ALLEN, JR.

Submitted in Partial Fulfillment
of the Requirements for the
Degree of Master of Science
at the
Massachusetts Institute of Technology

May, 1971

Signature of Author _____

Department of Nuclear Engineering
May 14, 1971

Certified by _____

Thesis Supervisor

Accepted by _____

Chairman, Departmental Committee on
Graduate Students

Archives



ASPECTS OF A SEISMIC STUDY OF THE MITR

by

George C. Allen, Jr.

Submitted to the Department of Nuclear Engineering on May 14, 1971, in partial fulfillment of the requirements for the Degree of Master of Science.

ABSTRACT

The design version of the Massachusetts Institute of Technology research reactor (MITR-II) was analyzed subject to earthquake forces. The problem was divided into three major areas.

First, the reactor core tank and support structure were studied. The reactor can be adequately cooled and shutdown if the core tank remains undamaged. Using a SABOR-5 computer program, the peak accelerations required to cause yielding of the core tank were calculated to be well above potential earthquake accelerations.

Second, the possibilities of potential damage to miscellaneous reactor systems were studied. The miscellaneous systems were studied to see if earthquake accelerations, resonance response, or differential motions would result in damage leading to major radioactive releases. No major potential hazards were discovered.

Third, the possibility of earthquake damage to the reactor stack was studied. An approximate analysis of the stack subject to dynamic earthquake shear and a 100 mile per hour wind was made. A case of a fallen stack was modeled to determine its effect on the containment building. The conservative calculations indicate that it is unlikely that the stack will fall and even if it were to fall onto the containment shell, it would not cause damage to the reactor core tank.

Within the scope of this report, it appears that the design MITR-II is adequate to provide required protection even in the event of the maximum expected earthquake motions.

Thesis Supervisor: David D. Lanning
Professor of Nuclear Engineering

ACKNOWLEDGEMENTS

The author wishes to express sincere appreciation for the assistance of his thesis supervisor, Professor David D. Lanning. He would also like to thank James Kotanchik who made available the results of several SABOR-5 computer code calculations. The author also thanks Edward Barnett and the reactor operations staff for their assistance.

The author would also like to acknowledge the valuable assistance of Professor J. M. Biggs and Professor R. J. Hansen of the Department of Civil Engineering, and the advice of Professor E. A. Witmer and Barbara Berg of the Department of Aeronautics and Astronautics. He is also grateful to Chris Ryan for loan of a Schaevitz accelerometer. Special thanks go to Miss Schmidt for her help in preparation of this document.

Many of the calculations in this thesis were made using the System 360/M65 of the M.I.T. Computation Center.

TABLE OF CONTENTS

	<u>Page</u>
Chapter 1. Seismology and Method of Analysis	10
1.1 Introduction	10
1.2 History of Earthquakes	10
1.3 Earthquake Zone and Return Period	12
1.4 Local Soil Conditions at the MITR-II Site	12
1.5 Analysis of the MITR-II	14
 Chapter 2. Analysis of the MITR-II Core Tank	 24
2.1 Introduction	24
2.2 Summary of Loads	24
2.2.1 Inner Vessel Loads	27
2.2.2 Outer Core Tank Loads	28
2.2.3 Calculational Model	29
2.3 Description of the SABOR-5 Computer Program	31
2.4 Outline of Analysis	32
2.5 Results of the Calculations	35
2.6 Determination of the Fundamental Frequency of the Water-Filled Core Tank	40
2.7 Analysis of Results	41
 Chapter 3. General Areas of Seismic Interest in MITR-II	 45
3.1 Introduction	45
3.2 Reactor Floor Design Loadings	45

	<u>Page</u>
3.3 Piping	49
3.4 Seismic Effect on Control Rods	50
3.4.1 Description of Control Rod Assembly	50
3.4.2 Drop Time	51
3.4.3 Rod Whip During an Earthquake	54
3.5 Building Penetrations	58
3.6 Seismic Instrumentation	64
3.7 Temporary Shield Walls	67
Chapter 4. Reactor Stack	69
4.1 Introduction	69
4.2 Approximate Earthquake Analysis of Stack	69
4.3 Worst Case of Stack Failure	74
4.3.1 Load Model	74
4.3.2 Calculational Model	74
4.3.3 Local Buckling of Roof	78
4.3.4 Results of SABOR-5 Analysis	78
4.4 Summary	80
Chapter 5. Summary	82
Appendix A - SABOR-5 Results of the Reactor Vessel	84
Appendix B - Fortran IV Computer Loads Program used on the Inner Flow Shroud	89
Appendix C - Fortran IV Computer Loads Program used on the Outer Core Tank	96

	<u>Page</u>
Appendix D - Fortran IV Computer Program used in Determination of Fundamental Frequency of Core Tank	102
Appendix E - Calculation of Fundamental Mode of Coolant Pipe	109
Appendix F - Calculation of Guide Tube Dis- placement from 1 g acceleration	111
Appendix G - Fortran IV Computer Program for Approximate Stack Analysis	113
Appendix H - References	117

LIST OF FIGURES

<u>Figure No.</u>	<u>Page</u>
1.1 Relations between intensity scales and acceleration	16
1.2 Seismic Probability Map of the United States I	17
1.3 Seismic Probability Map of the United States II	18
1.4 Seismic Probability Map of the United States III	19
1.5 Earthquake Intensity - Acceleration Relationships	20
1.6 Contour Map of Accelerations as a Percent of g with 100 year return period	21
1.7 Contour Map of Return Period in Years for Acceleration of 0.1 g	22
1.8 MITR-II Site Plan	23
2.1 Outer Core Tank	25
2.2 Inner Vessel and Flow Shroud	26
2.3 Orientation of Theta Positions of Core Tank Support	37
2.4 Calculated SABOR-5 Stresses	38
3.1 Reactor Floor Design Loadings	46
3.2 Simplified Representation of MITR-I Lattice	47
3.3 Control Rod Assembly	52
3.4 Rod in Control Rod Guide Tube	54
3.5 Model of Control Rod Displacement	57
3.6 Seismic Separation of Air Lock	59

<u>Figure No.</u>	<u>Page</u>
3.7 Accelerometer Signal Circuit	65
3.8 Accelerometer Output	66
4.1 Fallen Stack Zones	73
4.2 Model of Fallen Stack	76
4.3 Element Divisions of the Containment Roof	77
A.1 Freebody Diagram of Core Tank	86
D.1 Assumed Initial Displacements	108

LIST OF TABLES

<u>Table No.</u>	<u>Page</u>
2.1 Limiting Accelerations on Core Tank	39
3.1 Approximate Reactor Floor Loading from Lattice	48
3.2 Building Penetrations	61
4.1 Shear Stesses in Stack	71
4.2 Loads Used in Fallen Stack Problem	75
4.3 Stresses on Containment Roof from Fallen Stack	79
A.1 Static Case Comparisons of Calculations	85
A.2 Comparison of Static SABOR-5 Case with Free-body Diagram	85
A.3 Inner Vessel Stress	87
A.4 Outer Vessel Stress	88

Chapter 1

SEISMOLOGY AND METHOD OF ANALYSIS

1.1 INTRODUCTION

Earthquakes must be considered in the design of nuclear reactors, even in the New England area. Most earthquakes in New England pass without being noticed, for there are no less than several thousand minor earthquakes each year. The Massachusetts Institute of Technology research reactor (MITR-II) located in Cambridge, Massachusetts must be able to withstand earthquake motion without endangering the local populace. This work is an evaluation of major aspects of a seismic study of MITR-II.

The remainder of this chapter will cover the history of earthquakes in the Boston area and the seismic probability of the site area. The last section of this chapter will explain the seismic analysis sequence of MITR-II.

1.2 HISTORY OF EARTHQUAKES

The Cambridge area lies in the Boston Basin which has been relatively free of earthquakes in recorded times.(S1). The United States Department of Commerce in Earthquake History of the United States (H2) has the following to say about Massachusetts.

"In addition to feeling some of the more severe Canadian earthquakes and the New York and Grand Banks earth-

quakes of 1929, 17 (of intensity 5 and over on the Rossi-Forel scale) are listed for this state. In colonial times there were a large number of earthquakes in the northeast part of the state near Newburyport, and several of these, especially that of 1727 (75,000 square miles), were widely felt. That of 1755, near Boston, was felt over an area of 300,000 square miles. The shock of 1925 in the vicinity of Boston was strong. Numerous moderate shocks have been felt in the southeast part of the state."

Massachusetts earthquakes of Rossi-Forel intensity of seven or greater in Earthquake Damage and Earthquake Insurance by John R. Freeman (Fl) as follows:

Date	Location	Rossi-Forel Intensity
1638	Plymouth, Mass.	8
1662	Boston, Massachusetts	8
1727	Newburyport, Mass.	8
1744	Newburyport, Mass.	8
1755	Boston, Massachusetts	9
1817	Woburn, Massachusetts	8

An explanation of the Rossi-Forel scale and a correlation with the Modified-Mercalli intensity scale is found in Figure 1.1. Historical accounts of Boston area earthquakes during 1727-1755 included such phrases as (H1):

"...many chimneys were leveled with the roofs of the houses, and many more shattered and thrown down in parts..."

"...the gable ends of some brick buildings (were) thrown down and others cracked..."

"...(strong motions) continued about two minutes..."

1.3 EARTHQUAKE ZONE AND RETURN PERIOD

At the present time there is no standard Seismic Risk or Probability Map available on the United States that an engineer is required to follow. Such maps do however give a feel for the potential damage or expected maximum intensity in a given area. Examples of three Seismic Risk maps are shown in Figures 1.2, 1.3, and 1.4. From these maps, the Cambridge MITR-II site appears to be in a region of moderate potential earthquake damage and have a maximum earthquake intensity of about 8 on the Modified-Mercalli scale. The relationship between Modified-Mercalli intensity and acceleration is shown in Figure 1.5.

A different representation of earthquake activity is shown by the use of return periods (approximate frequency) of various accelerations in Figures 1.6 and 1.7. The predicted return period for a 0.1 g. earthquake (equivalent to VII on the Modified-Mercalli scale) for a Cambridge site would be approximately 1,000 years according to the maps of Milne and Davenport (1969).

1.4 LOCAL SOIL CONDITIONS AT THE MITR-II SITE

The average soil conditions at the site are about 11 feet of miscellaneous fill overlying from 5 to 10 feet of soft organic silt and peat. Immediately below are approximately 10 feet of hard, medium to fine sand and gravel lying above more than 100 feet of Boston blue clay. The

reactor building and adjacent stack, as shown in Figure 1.8, are on reinforced concrete mats founded on the hard sand and gravel (A1).

In general, earthquake motions are amplified and otherwise modified by near-surface geological features. At other locations, in a study by Tamura (H1) it was found that the peak acceleration at ground surface was about twice the peak acceleration at a depth of 300 meters (the same trend of increased motion from depth up to the surface occurred for both a deposit of soil and rock). Based on the assumption that most ways of estimating ground motions really apply for a very dense hard alluvium or for soft rock, Newmark and Hall suggested site factors to modify earthquake motions to make them apply for very soft ground or hard rock (H1).

Newmark's Site Factors

Soft Ground	1.5
Firm soil - Soft rock	1.0
Hard rock	0.67

The MITR-II is located on soft ground. Assuming a reasonable design peak acceleration of 0.15 g. based on the area history and on the predicted return periods (Boston Edison's Plymouth Nuclear Power Station used approximately 0.15 g. as its design peak acceleration) and applying Newmark's site factor of 1.5, the estimated design peak earthquake acceleration at the MITR-II site would be 0.225 g.

1.5 ANALYSIS OF THE MITR-II

The reactor shield is an integral unit with the remainder of the building. The building rests on a 70 foot diameter, 3 feet thick, heavily reinforced concrete pad. It is expected that the shield and pad will shift as a unit rather than cracking under seismic shock. On a more quantitative basis, a careful review of the seismic effects on the MITR-II has been made with the assistance of Professor Robert J. Hansen and Professor John M. Biggs from the Civil Engineering Department of MIT. Based on their experience with seismic effects, (H1) it was concluded that the support for the main core tank of the MITR-II will not lose its structural integrity and hence will always be able to support the core tank. As shown in the MITR-II Safety Analysis Report (S1), the reactor can be shut down by insertion of independently acting shim blades or by backup shutdown action of dumping the D O reflector. It has also been shown in the MITR-II Safety Analysis Report that the core will be adequately protected as long as H₂O remains in the tank for natural convective cooling after the controls actuate to shut the reactor down. One problem which is particularly severe in regions of high seismic activity in the western United States but can be ignored for the MITR-II site, is the possibility of fault displacement through the site (H1).

Chapter II of the following report, contains a detailed

analysis to determine the earthquake forces that would be required to cause a yield stress in the core tank itself. The core tank is analyzed for the operating case with the D₂O reflector dumped, being subject to various accelerations.

Chapter III discusses a study of seismic effects on several reactor systems such as control rods, miscellaneous piping, building penetrations, and floor loadings.

Chapter IV is seismic study of the brick stack adjacent to the reactor building.

Chapter V is a summary and list of potential recommendations.

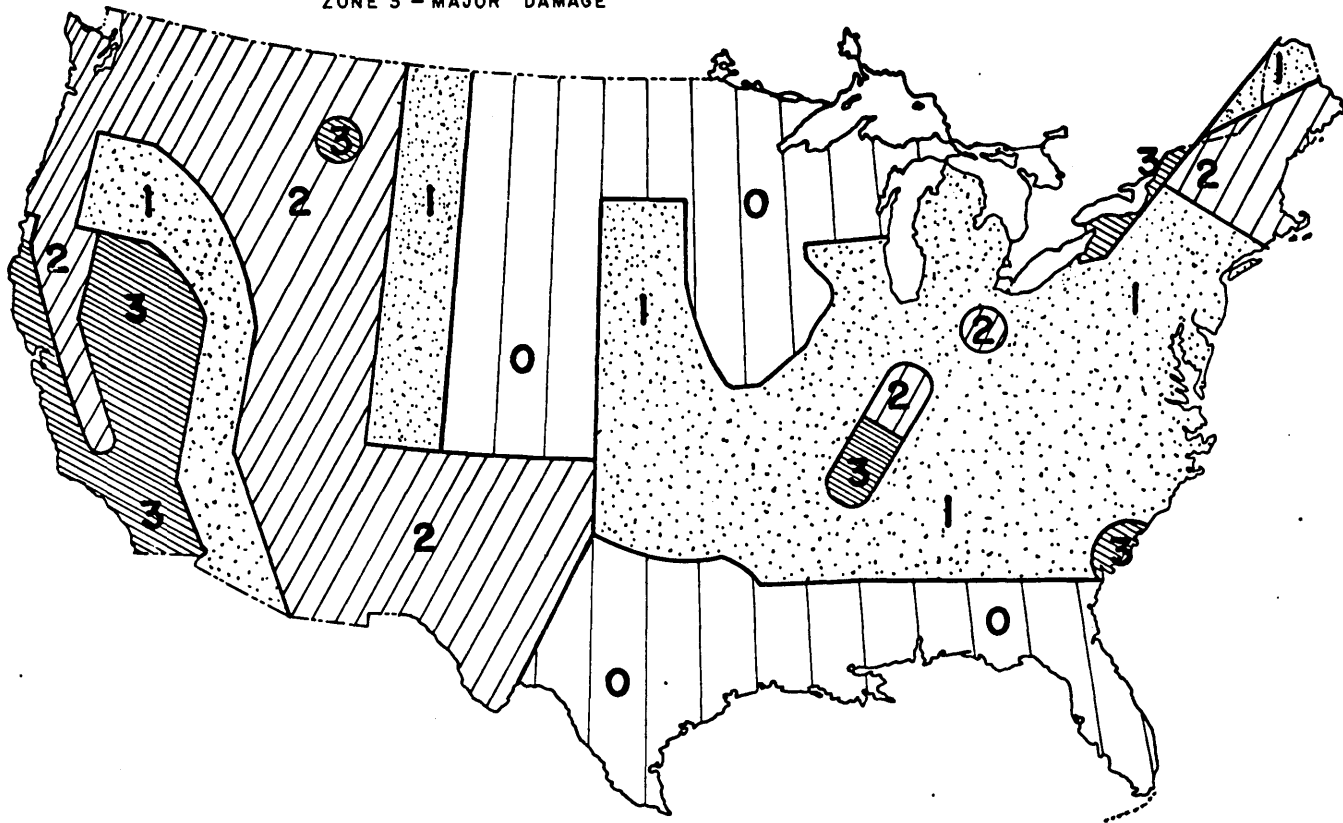
FIGURE 1.1
RELATIONS BETWEEN INTENSITY
SCALES AND ACCELERATION

ROSSI-FOREL INTENSITY SCALE (1883)	MODIFIED-MERCALLI INTENSITY SCALE (1931), WOOD AND NEUMANN I	GROUND ACCELERATION a
COL. 1	COL. 2	COL. 3
	I Detected only by sensitive instruments.	$\frac{cm}{sec}$ $\frac{a}{g}$
I The shock felt only by experienced observer under very favorable conditions.	II Felt by a few persons at rest, especially on upper floors; delicate suspended objects may swing.	2
II Felt by a few people at rest, recorded by several seismographs.	III Felt noticeably indoors, but not always recognized as a quake; standing autos rock slightly, vibration like passing truck.	3 4 5 .005g 6 7 8 9 10 .01g
III Felt by several people at rest; strong enough for the duration or direction to be appreciable.	IV Felt indoors by many, outdoors by a few; at night some awakened; dishes, windows, doors disturbed; motor cars rock noticeably.	
IV Felt by several people in motion; disturbance of movable objects, cracking of floors.	V Felt by most people; some breakage of dishes, windows, and plaster; disturbance of tall objects.	20 30
V Felt generally by everyone; disturbances of furniture, ringing of some bells.	VI Felt by all; many frightened and run outdoors; falling plaster and chimneys; damage small.	40 50 .05g 60 70 80 90 100 .01g
VI General awakening of those asleep, ringing of bells, swinging chandeliers, startled people run outdoors.	VII Everybody runs outdoors; damage to buildings varies, depending on quality of construction; noticed by drivers of autos.	
VII Overthrow of movable objects, fall of plaster, ringing of bells, panic with great damage to buildings.	VIII Panel walls thrown out of frames; fall of walls, monuments, chimneys; sand and mud ejected; drivers of autos disturbed.	200 300
VIII Fall of chimneys; cracks in walls of buildings.	IX Buildings shifted off foundations, cracked, thrown out of plumb; ground cracked; underground pipes broken.	400 500 .05g 600 700 800 900 1000 1g
IX Partial or total destruction of some buildings.	X Most masonry and frame structures destroyed; ground cracked; rails bent; landslides.	
X Great disasters, ruins; disturbance of strata, fissures, rockfalls, landslides; etc.	XI New structures remain standing; bridges destroyed; fissures in ground; pipes broken; landslides; rails bent.	2000 3000
	XII Damage total; waves seen on ground surface; lines of sight and level distorted; objects thrown up into air.	4000 5000 .5g 6000

(N1)

FIGURE 1.2

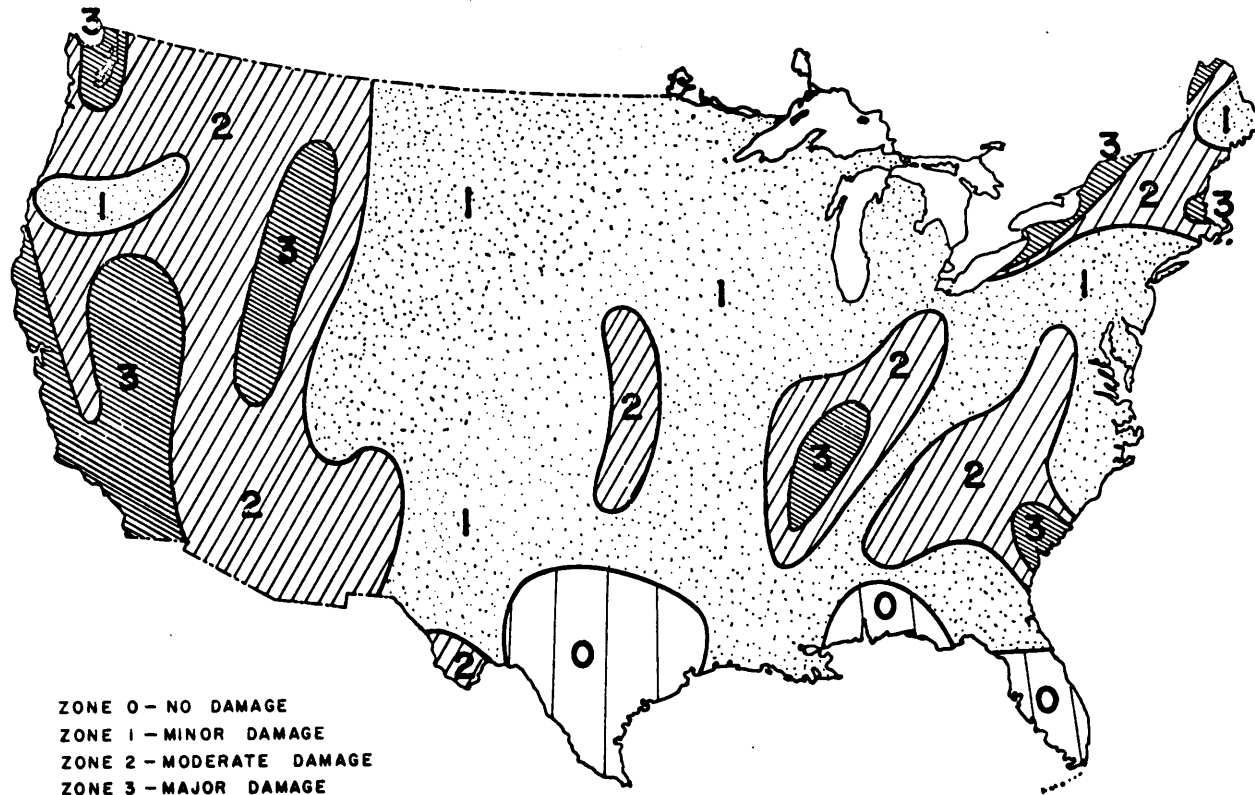
ZONE 0 - NO DAMAGE
ZONE 1 - MINOR DAMAGE
ZONE 2 - MODERATE DAMAGE
ZONE 3 - MAJOR DAMAGE



SEISMIC PROBABILITY MAP OF THE UNITED STATES I

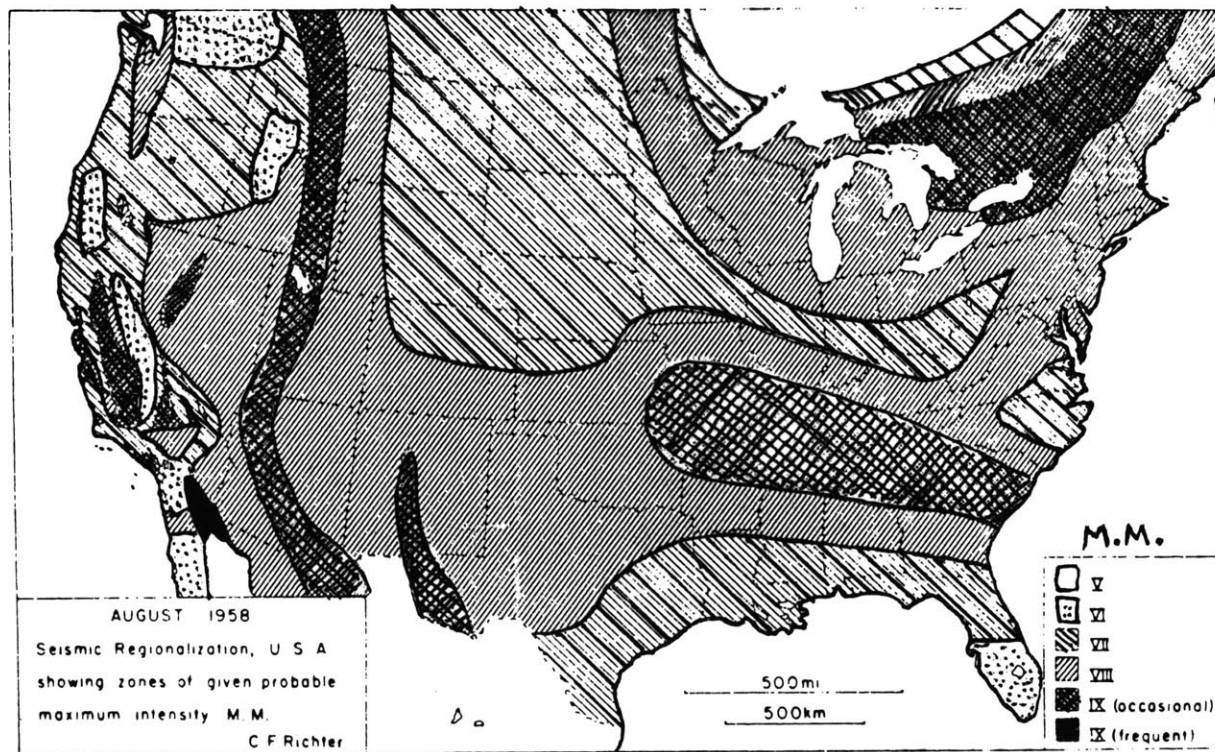
(HI)

FIGURE 1.3



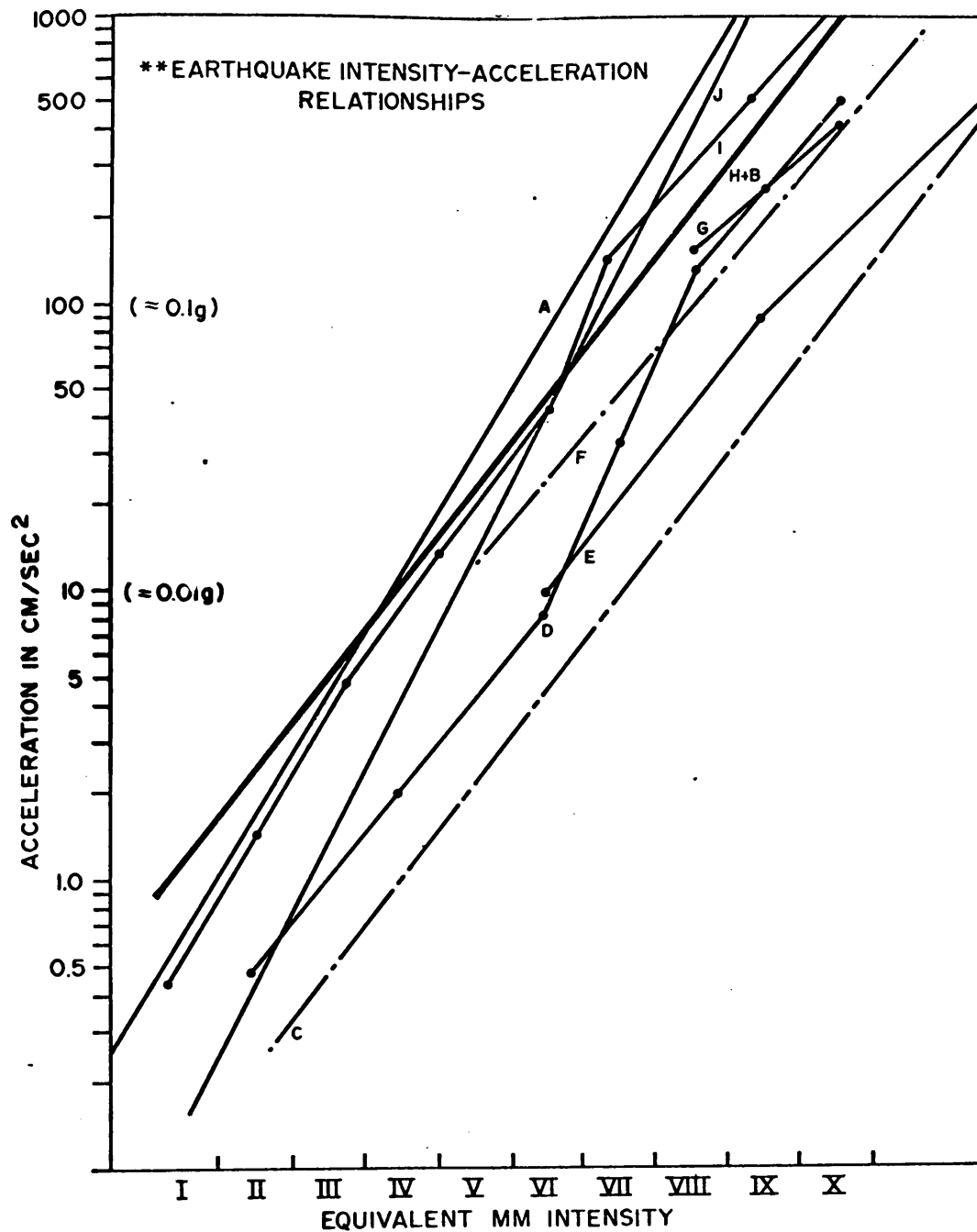
SEISMIC PROBABILITY MAP OF THE UNITED STATES II
(HI)

FIGURE 1.4



SEISMIC PROBABILITY MAP OF THE UNITED STATES-III
(HI)

FIGURE 1.5



A - HERSHBERGER (1956)
 B - GUTENBERG & RICHTER (1942)
 *C - CANCANI (1904)
 *D - ISHIMOTO (1932)
 *E - SAVARENSKY & KIRNOS (1955)

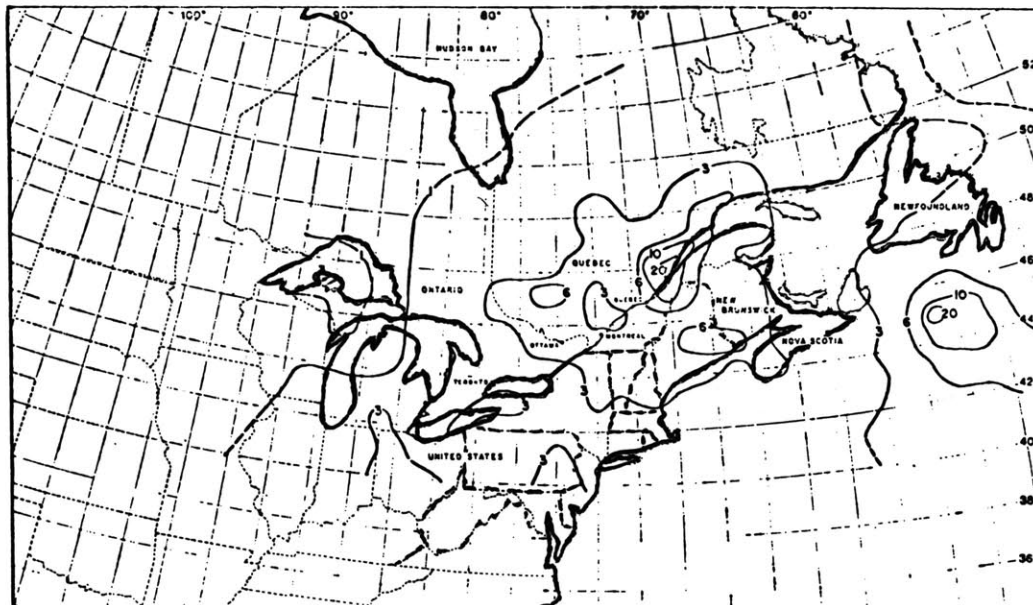
*F - MEDVEDEV ET AL. (1963)
 *G - N.Z. DRAFT BY-LAW
 H - TID-7024 (1963)
 *I - KAWASUMI (1951)
 *J - PETERSCHMITT (1951)

**DATA COMPILED BY WESTON GEOPHYSICAL ENGINEERS

* DATA FROM G. A. EIBY (1965)

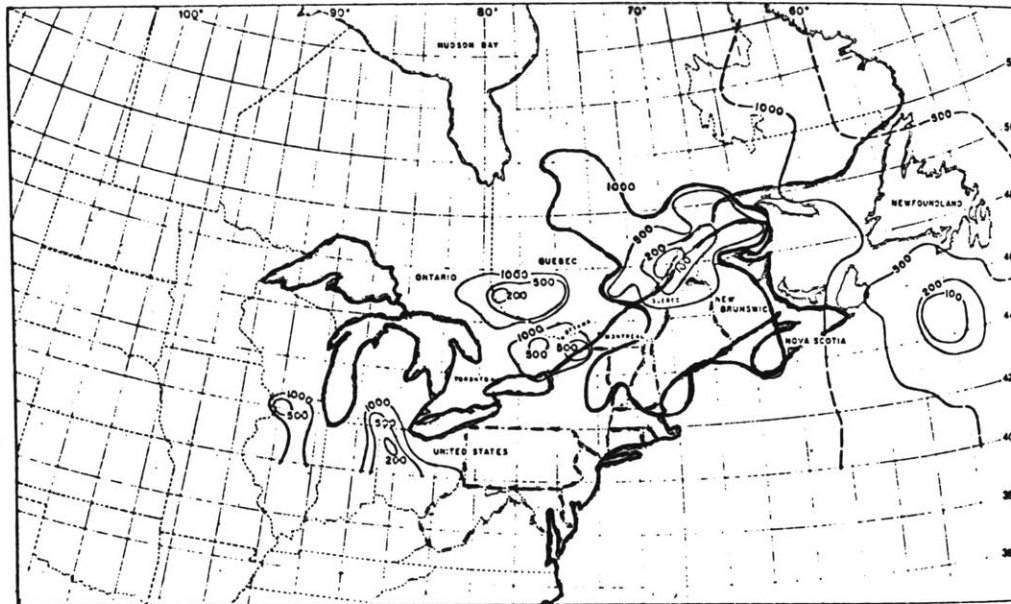
(H I)

FIGURE 1.6



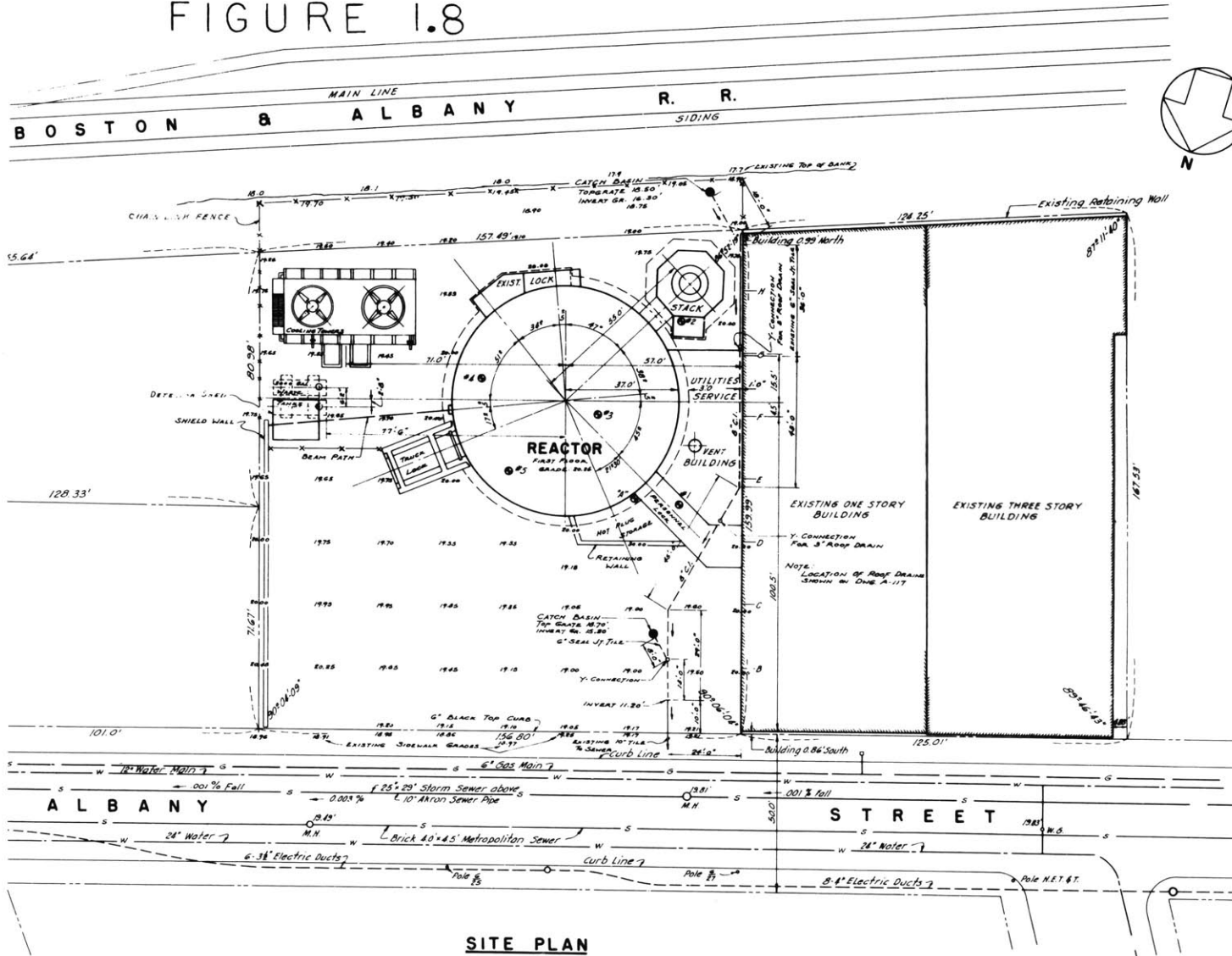
CONTOUR MAP OF ACCELERATIONS AS A PERCENT OF
OF g WITH A 100 YEAR RETURN PERIOD FOR EASTERN
CANADA (from Milne and Davenport, 1969)

FIGURE 1.7



CONTOUR MAP OF RETURN PERIOD IN YEARS FOR
ACCELERATION OF 0.1 g IN EASTERN CANADA
(from Milne and Davenport, 1969)

FIGURE 1.8



SITE PLAN

Chapter 2

ANALYSIS OF THE MITR-II CORE TANK

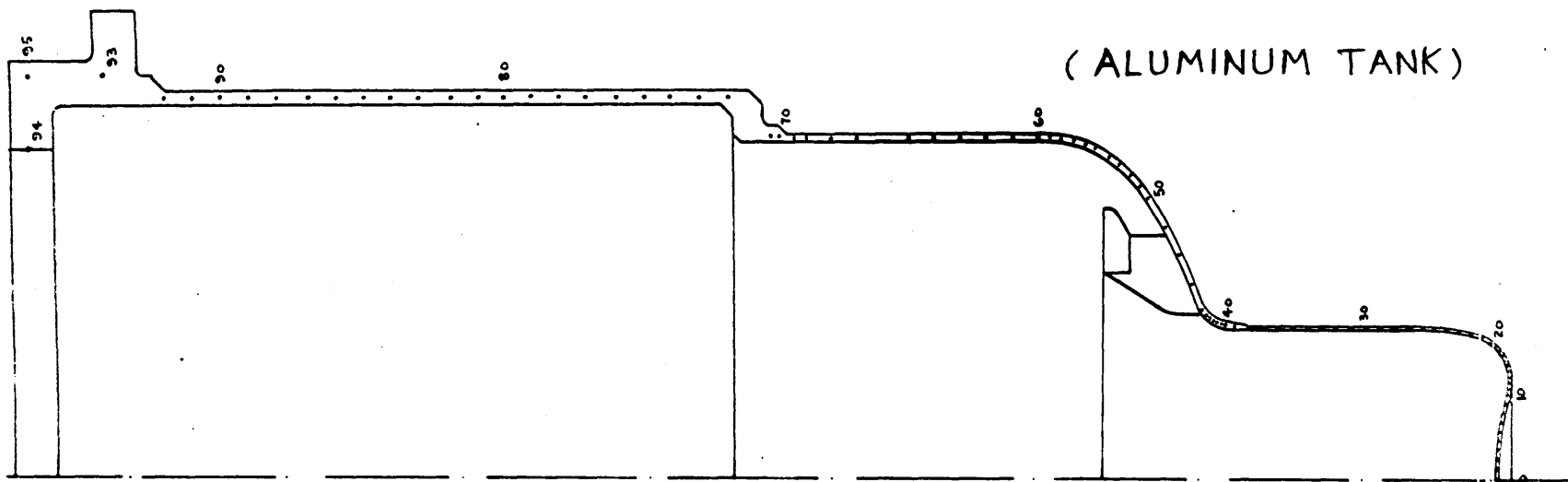
2.1 INTRODUCTION

The critical component of the MITR-II subject to seismic effects is the reactor vessel. Because of the extremely rigid structure supporting the reactor vessel, earthquake motion of the reactor vessel supports will be similar to soil motions at the foundation mat of the reactor building. The reactor can be maintained in a safe condition and the fuel adequately cooled if the core tank is not damaged and remains filled with water. Considering the reactor core tank as the critical component to be maintained, independent of the need of the outer containment building; failure of the stack or mechanical support facilities from earthquake motion can be tolerated, even in the unlikely case of the stack falling and hitting the outer containment building.

2.2 SUMMARY OF LOADS

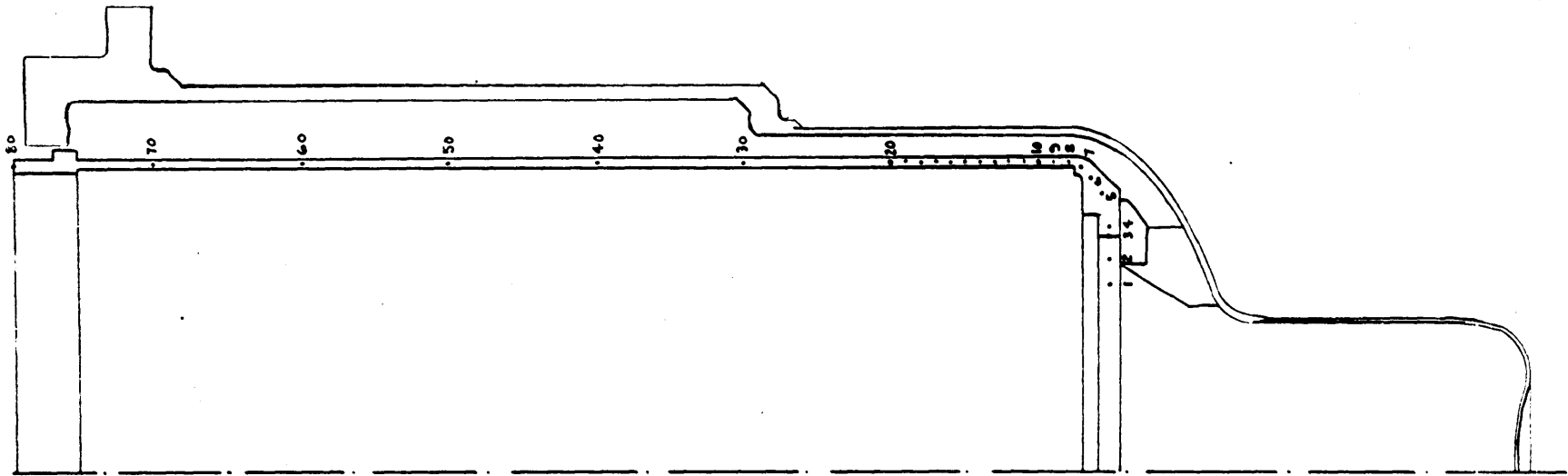
The configuration of the reactor core tank is shown in Figure 2.1 and the configuration of the inner vessel (flow shroud) is shown in Figure 2.2. Studies have been made of both the H₂O outer core tank and the inner vessel, including the flow shroud, to determine stress levels in each structure in terms of several loading parameters.

The complete set of loads consists of a gravity load and inertia loads that might be associated with both vertical



OUTER CORE TANK
 ELEMENT DIVISIONS FOR SABOR-5 CALCULATIONS

FIGURE 2.1



INNER VESSEL AND FLOW SHROUD
ELEMENT DIVISIONS FOR S A B O R - 5 CALCULATIONS

FIGURE 2.2

and horizontal seismic motion of the structure. For all cases, the vertical acceleration was set at 2/3 of the horizontal level, following the suggestion of Professor Hansen of the MIT Civil Engineering Department. The discussion of the loads given below will be divided into two sections: (1) loads for the inner vessel; and (2) loads for the outer core tank.

2.2.1 Inner Vessel Loads

The loads associated with the inner vessel and flow shroud must be considered in terms of its geometry. The fuel element hexagonal container is porous and hence no water inertial loads are acting upon it. The support ring of the fuel element container will be subject to water and structural inertial loads only, but no hydrostatic loads since both the inner vessel and outer core tank are connected. Loads on the vertical section of the flow shroud are due to the inertia of the metal itself and the inertial loads due to the contained water. These inertial loads can be characterized by the expression (for the horizontal component).

$$\begin{aligned}
 F &= \rho_w R_i \cos\theta \quad -90^\circ \leq \theta \leq 90^\circ \\
 &= 0 \quad \quad \quad 90^\circ \leq \theta \leq 270^\circ \quad (2.1)
 \end{aligned}$$

where ρ_w = density of water

R_i = inside radius of the inner vessel

θ = angle measured from the direction of horizontal motion. (The orientation of is shown in Figure 2.3).

The above set of loads is conveniently represented using

4 terms of a Fourier cosine series which yields the expression:

$$F = 0.31831 P_w R_i + 0.5 P_w R_i \cos \theta + 0.21221 P_w R_i \cos 2\theta - 0.04244 P_w R_i \cos 4\theta \quad (2.2)$$

This form returns 99% of the peak load and is an adequate representation of the load for this study.

The effect of the various loads have been calculated by using a computer program SABOR-5 (K2).

For convenience in running the SABOR-5 program, a small program was written to generate a set of loads as the input for SABOR-5. A listing of this program is included in Appendix B.

When SABOR-5 is run for the inner vessel, the program considers the nodes at which the inner vessel is supported by the outer core tank to be restrained, and it calculates a set of forces to be applied to the outer vessel at the corresponding outer vessel nodes.

The effect of the fuel elements and their supporting material is included by considering that portion of the structure as a lumped mass at its center of gravity, and equivalent ring loads are calculated and applied at the edge of the support flange.

2.2.2 Outer Core Tank Loads

Because of the narrow clearance between the flow shroud and the core tank, water inertial loads resulting from sideways motion are neglected. In the lower portion of the

vessel, the contribution of the water inertial load is small, (due to the small local radius and the large portion occupied by the core) and can be neglected in comparison to the loads due to the very large contribution from the upward motion and the hydrostatic head.

For the core tank, a small program was again written to provide the input to SABOR-5. A listing of this program is included in Appendix C.

2.2.3 Calculational Model

The reactor vessel is composed of two major components, the outer core tank and the inner flow shroud. In the calculational model, the outer core tank was divided into 94 finite elements and the inner flow shroud was divided into 79 finite elements. The stress on each of these elements was determined by using the SABOR-5 computer program. These elements are shown in Figures 2.1 and 2.2.

Several problems were encountered in the modeling and in the calculation of loads. Primary among these is the problem associated with the support geometry between the inner vessel and the outer core tank. The physical support consists of 12 feet equally spaced circumferentially between the inner and outer vessel. This construction introduces physical asymmetry into the geometry and since SABOR-5 handles asymmetric geometries only with great difficulty, some study of the modeling of the structure in that area was made.

SABOR-5 models all geometries as axisymmetric structures. Local asymmetries are modeled by "smearing" the structure in that local area. For structural elements such as the twelve supporting feet, the SABOR-5 program would generate results for a continuous ring between the inner and outer vessels (equivalent to increasing the metal density by appropriate amounts for the elements in the feet area). But in this model, serious errors can result in the calculated local stress distribution in the area where the feet rest upon the outer core tank, and for this reason a detailed study of this problem was undertaken.

For this detailed study, the SABOR-5 calculated loads at the feet of the inner vessel were lumped into values at each of the twelve feet and a higher order Fourier series loading for the outer core tank was computed from them. Harmonics 0, 1, 11, 12, 13, 23, 24, 25, 35, 36 were used. This representation of the load at the feet was within 5% of the exact value, and the load midway between the feet was negligible. The local stress distribution in the region of feet on the outer vessel was then computed. The values obtained were compared with those of the continuous mode. This comparison yielded the result that the peak stresses were nearly 50% greater than those obtained from a continuous model of the support loads.

The two maximum stress locations on the outer tank were

located near the bottom center of the tank and in the feet area at the element above the feet. Thus to be conservative, the feet area stresses reported in Appendix A are the maximum stresses in the feet area calculated using the continuous case and increased by a factor of 60%.

2.3 DESCRIPTION OF THE SABOR-5 COMPUTER PROGRAM

The analysis by using the SABOR-5 Computer Program treats linear-elastic, static, load-deflection behavior of meridionally-curved, variable thickness double - and/or single-layer, branched thin shells of revolution which may be subjected to concentrated or distributed external mechanical and/or thermal loads. In the present analysis, it is assumed that the structure is axisymmetric in terms of both geometry and material properties; hence, when the structural deformations are expressed as sums of Fourier harmonics of the circumferential coordinate Θ , the equilibrium equation for the structure consists of a set of harmonically-uncoupled load-displacement equations (ie., there is a separate set of equations for each harmonic of the structural response). (K1). The harmonic deflection coefficient may be determined by solving these equations for each significant loading harmonic present, and may then be summed to obtain the complete deformation. The requirement of material axisymmetry means that while nonuniform and/or asymmetric temperature distributions may be treated,

the material properties, E, ν, α , must be independent of the local temperature, but more precisely independent of location .

2.4 OUTLINE OF THE ANALYSIS

The application of the discrete-element procedure may be divided into three phases: structural idealization, evaluation of element properties, and analysis of the complete structure. In the analysis of both the inner and outer vessels, the structures were modeled as single-layer elements.

In the discrete-element formulation, the actual structure is replaced by an assemblage of geometrically-compatible discrete elements. As previously stated, for the present analysis, the basic discrete elements to be employed are single-layer. For a single-layer element only four quantities are necessary to fully describe the state of deformation within an element. These quantities for each element are:

- (a) Midsurface meridional displacement, μ
- (b) Midsurface circumferential displacement, V
- (c) Normal displacement, W
- (d) Total meridional rotation, $\frac{\partial W}{\partial s} + \mu \frac{\partial \phi}{\partial s}$

In the above expressions ϕ is the meridional slope of the element. One may reduce the number of degrees of freedom necessary to describe the deformation state of each element by choosing a set of generalized displacements corresponding

to the nodal values of the displacements in each element. Then the choice of a reasonable assumed (analytic) function for the interior displacements, which also includes inter-element displacement compatibility, provides a complete representation of the overall deformation state of the element.

At the bounding nodes of the P^{th} element (say nodes q and r) let generalized forces $Q_{1,q} \dots Q_{n,q}, Q_{1,r} \dots Q_{n,r}$ (where $n=4$ for single-layer elements) be defined corresponding to the generalized displacements at the node. The application of the Principle of Stationary Total Potential Energy yields the equations for static equilibrium for the P^{th} element; as a consequence of the condition of structural axisymmetry, these force-displacement relations are harmonically uncoupled. In matrix form, the force-displacement relation for the j^{th} harmonic A-series Fourier displacement component becomes:

$$[K_p^{(j)}] \{q_p^{(j)}\} = \{Q_p^{(j)}\}$$

where $[K_p^{(j)}]$ is the element stiffness matrix. Imposition of nodal compatibility at interior nodes of the complete structure requires that at an interior node r , bounded by elements p and q the following relationship must be satisfied:

$$\left. \begin{matrix} q_{1,r} \\ q_{2,r} \\ \vdots \\ q_{n,r} \end{matrix} \right\} = \left. \begin{matrix} q_{1,r} \\ q_{2,r} \\ \vdots \\ q_{n,r} \end{matrix} \right\} \quad (2.3)$$

P^{th} element q^{th} element

The total potential energy (Π_p) for the n discrete elements, including the strain energy as well as the potential energy of all of the virtual-work-equivalent nodal loads (for both distributed and ring loads), and the imposition of nodal compatibility then becomes expressed in terms of the N independent nodal displacement of the complete assembled discretized structure. The equilibrium equations for the entire structure are then obtained by setting $\delta \Pi_p = 0$, where only displacement variations are permitted. For the j^{th} harmonic A-series Fourier displacement harmonic, for example, these read:

$$\begin{array}{ccc} [K^{(j)}] \{ q^{(j)} \} & = & \{ F^{(j)} \} \\ N \times N & N \times 1 & N \times 1 \end{array} \quad (2.4)$$

In the above equation, N is the total number of degrees of freedom associated with the complete structure, and the i th term $F_i^{(j)}$ of the generalized force vector is the sum of all the j^{th} harmonic generalized forces from all the individual discrete elements and from the j^{th} harmonic generalized ring-type loads, both of which are associated with i th degree of freedom of the complete assembled discretized structure. Also, $[K^{(j)}]$ represents the (assembled) stiffness matrix for the complete structure.

For most practical applications, the physical structure will be restrained in some fashion such that one or more generalized displacements will be known before the general solution is obtained. A solution for the complete

displacement field then will not be found from Equation (2.4) but from a reduced equation from which the restrained degrees of freedom have been deleted. The reduced equation is similar in form to Equation (2.4) and follows:

$$\begin{matrix} [K^{(j)}] & \{ q^{(j)} \} & = & \{ F^{(j)} \} & (2.5) \\ (N-R) \times (N-R) & (N-R) \times 1 & & (N-R) \times 1 & \end{matrix}$$

where R is the number of known or prescribed generalized displacements.

Equation (2.5) may be solved for the unknown-generalized displacements using any appropriate method. A similar equation may be written for each loading harmonic present. The total generalized displacement may then be found by summing the contributions due to each loading harmonic. Since all of the N displacements are now known, they may be used to determine other information such as:

- (a) strains by use of the appropriate strain displacement relations and
- (b) stresses and/or stress resultants.

The detailed loads programs required to carry out the above - outlined discrete-element analysis for the specific case of the MITR-II reactor core tank and inner flow shroud are included in Appendices B and C. There are no thermal loadings in our analysis.

2.5 RESULTS OF THE CALCULATIONS

SABOR-5 gave results at the midplane, inner and outer

surfaces of each element of the vessels being analyzed for various circumferential theta stations. Comparison of the computer results with hand calculations showed agreement between the two methods (the computer method appears to be the more conservative). This comparison was made for the case of zero acceleration, static operating conditions (Table A.1). SABOR-5 also showed agreement between the static case and freebody stress analysis (Table A.2). On the basis of this agreement and from previous experience with the SABOR-5 program as documented in the work by Witmer and Kotanchik, (W1) the program is taken to give valid estimates of the stresses.

Extremely small stresses were calculated to occur in the inner flow shroud (Table A.3), in comparison with the outer core tank. The outer core tank is therefore shown to be the critical part.

The outer core tank has been analyzed for the following four cases:

- (a) static operating case (STC)
- (b) STC + 0.5 g. horizontal + 0.33 g. vertical
- (c) STC + 1.5 g. horizontal + 1.0 g. vertical
- (d) STC + 4.5 g. horizontal + 3.0 g. vertical

The peak stresses occurred on the inside of station 50 (Figure 2.1). This peak stress is actually the peak stress as given by the continuous case increased by a factor of 60%. The summary of the calculated results are in Table A.4.

FIGURE 2.3

ORIENTATION OF \oplus POSITIONS WITH
RESPECT TO THE DIRECTION OF
ACCELERATION OF CORE TANK
SUPPORT

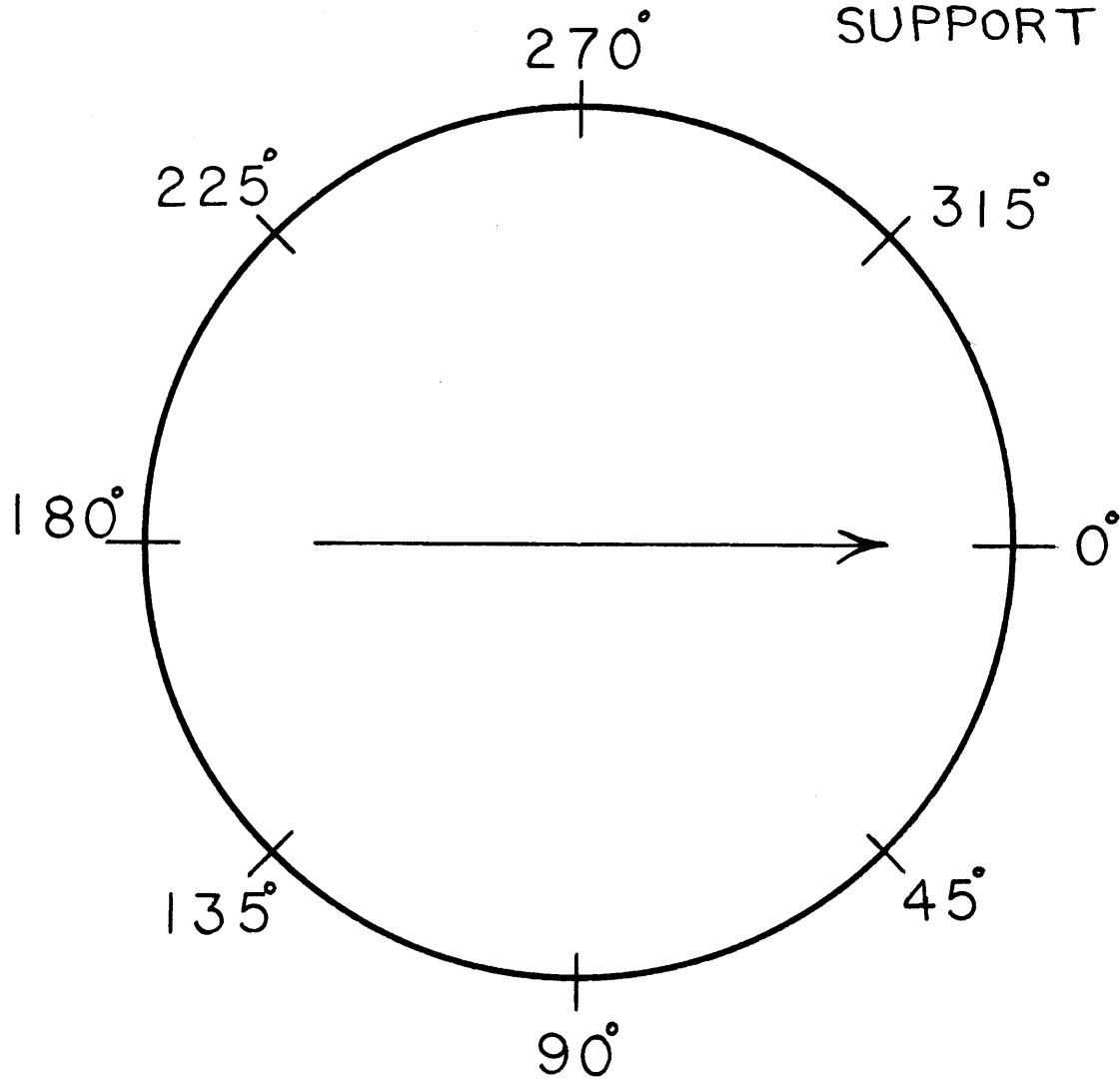


FIGURE 2.4

CALCULATED SABOR - 5 STRESSES

RESULTS FROM VARIOUS ACCELERATIONS
OF THE OUTER H₂O CORE TANK

- △ - G₀
- - G_s
- - G_s FEET (G_s + 0.6 G_s)

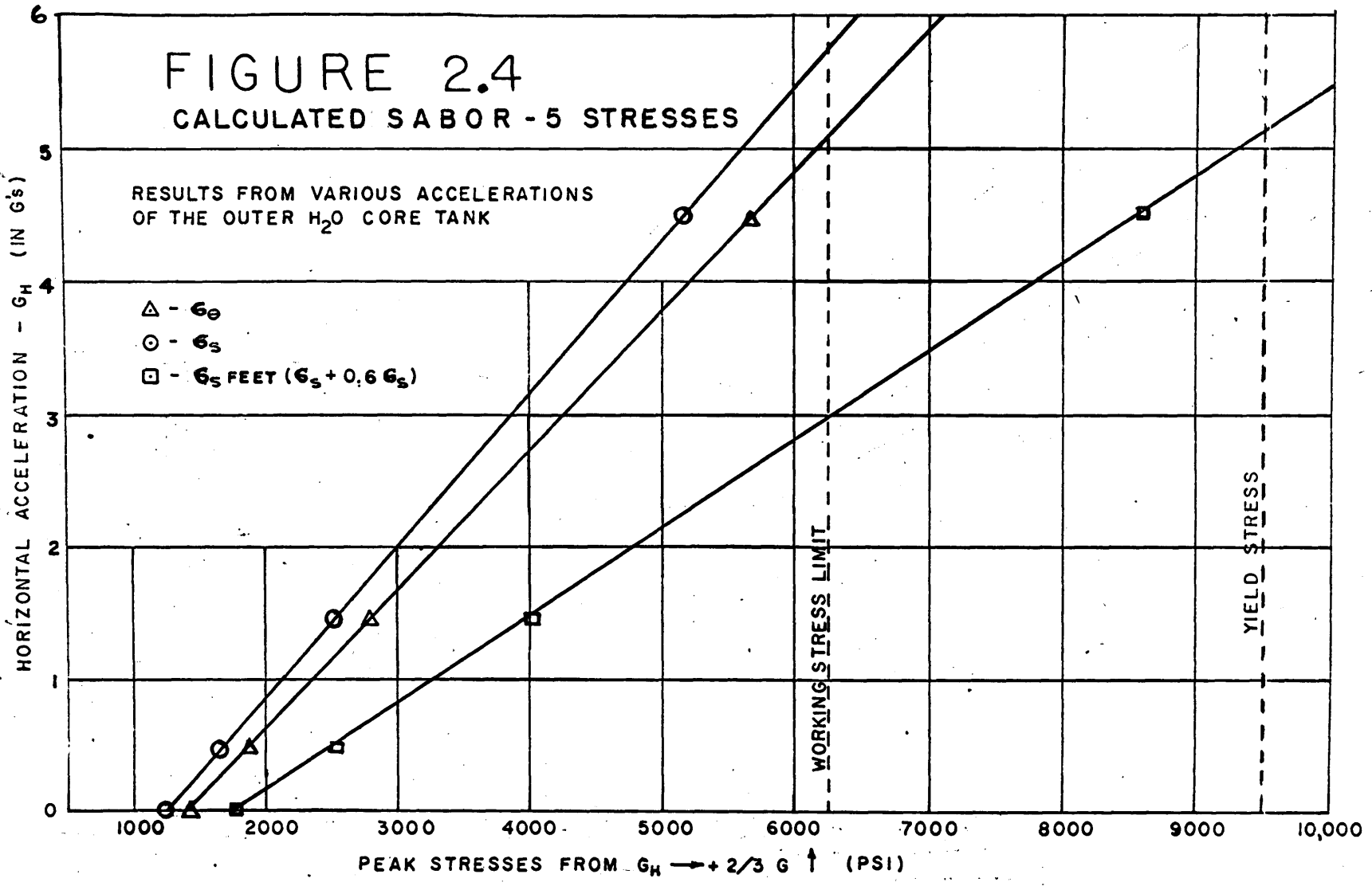


Table 2.1

LIMITING ACCELERATIONS ON CORE TANK

<u>Criteria</u>	<u>Horizontal Acceleration</u>	<u>Vertical Acceleration</u>
Peak Stress		
= working stress limit (6250 psi)	2.9 g	2.0 g
Peak Stress		
= yield stress (9500)	5.1 g	3.4 g

The analysis showed that stress increased linearly with acceleration (Figure 2.4). Thus, by extrapolation of the results to the condition for which the peak stress equals the working stress, and the case where the peak stress equals the yield stress, the limiting accelerations were derived as shown in Table 2.1.

2.6 DETERMINATION OF THE FUNDAMENTAL FREQUENCY OF THE WATER FILLED CORE TANK

The fundamental mode of the water-filled core tank is determined by a numerical iterative method commonly known as the Stodola and Vianello method (H3). For a structural system the following equation holds.

$$\bar{K} \bar{U} = w^2 \bar{M} \bar{U} \quad (2.6)$$

where

\bar{K} = stiffness matrix

\bar{U} = displacement matrix

\bar{M} = mass matrix

w = frequency of the mode corresponding to the displacement U

Rearranging terms

$$\frac{1}{w^2} \bar{U} = \bar{K}^{-1} \bar{M} \bar{U} \quad (2.7)$$

letting

$$\lambda = \frac{1}{w^2} \quad \text{and} \quad \bar{K}^{-1} \bar{M} = \bar{a} \quad (2.8)$$

then the Stodola and Vianello method can be used to solve

an equation of the form:

$$\bar{a} \bar{x} = \lambda \bar{x} \quad (2.9)$$

where after assuming an initial displacement, the process is iterated until λ converges on a maximum and thus obtaining the smallest natural frequency. The mass matrix and stiffness matrix are obtained by running the SABOR-5 program for the outer core tank. A computer program was written to convert the SABOR-5 mass and stiffness matrix to the X-Y-Z coordinate system and to increase the mass matrix by appropriate lumped masses corresponding to the water in the tank. The program also performs the inversion of the stiffness matrix and performs the iteration process for an inputted assumed original normalized displacement (a listing of this computer program is included in Appendix D.) After 101 iterations the solution had converged on:

$$24.8 \text{ cycles/sec.} = \text{1st mode of water filled core tank}$$

Thus resonant amplification does not appear to be a problem. (The initial assumed displacements are shown in Figure D.1)

2.7 ANALYSIS OF RESULTS

A detailed analysis has been made to determine the earthquake forces that would be required to cause a yield stress in the core tank itself. Vector forces on the tank were considered to be largest in the horizontal direction and a force of 2/3 of the horizontal force was simultaneously

applied downward (upward acceleration) in the vertical direction. The results of these calculations indicate that a combined horizontal acceleration of 5.1 g. and a vertical acceleration of 3.4 g. will cause a peak stress near the feet area of the core tank of 9500 psi which is equal to the yield stress limit for the aluminum tank.

It should be noted that these conclusions apply to the reactor structure and reactor core tank. It is conceivable that the effect of an earthquake could cause some damage to the reactor piping or building structure at lower accelerations; however, the action of the antisiphon valves would prevent a loss of the necessary H₂O coolant in the main core tank.

A summary of conclusions reached on the seismic effects has been prepared by Professor Biggs of the MIT Department of Civil Engineering who states that:

"Based upon the seismic criteria commonly used for nuclear power plants, the Design Basis Earthquake for the Cambridge area would probably have a maximum acceleration of about 0.2 g. This estimate considers both the seismicity of the region and the fact that Cambridge is an area of relatively soft soil conditions.

"The structure supporting the research reactor is a massive, rigid concrete block extending from the bottom of the foundation to the point of reactor vessel support. Therefore there would be little, if any, amplifications of

the acceleration in the structure itself, i.e., the acceleration at the reactor support would be essentially the same as at the bottom of the foundation.

"However, since the support system is a mat foundation on relatively soft soil, a certain degree of soil-structure interaction is to be expected. This tends to increase the fundamental period of the structure and to make the motion of the foundation somewhat different than that occurring in the undisturbed soil.

"The soil-structure interaction in this case would be almost entirely swaying, or horizontal shearing, in the soil. This type of behavior involves very high damping. As a consequence, there would be little amplification of the ground acceleration, i.e., the maximum acceleration of the rigid foundation would be essentially the same as that predicted for the ground, or 0.2 g.

"The natural period of the reactor vessel is very short compared to that of the soil-structure foundation system. Therefore, there is no possibility of resonance between the vessel and the supporting structure.

"All of the above leads to the conclusion that the maximum response acceleration of the reactor could be only slightly greater than the maximum ground acceleration of 0.2 g.

"It has been computed that the reactor is capable of withstanding (at yield stresses) static forces corresponding

to 5.1 g. horizontal acceleration and simultaneously 3.4 g. vertically. It is not conceivable, even under the most unfavorable circumstances, that the response to earthquake motions would be more than a small fraction of these amounts."

Chapter 3

GENERAL AREAS OF SEISMIC INTEREST IN MITR-II

3.1 INTRODUCTION

Many miscellaneous areas of seismic concern exist in a nuclear facility. The following areas of the MITR-II will be covered in this report chapter:

1. Reactor Floor Design Loadings
2. Control Rods
3. Piping
4. Building Penetrations
5. Seismic Instrumentation
6. Temporary Shield Walls

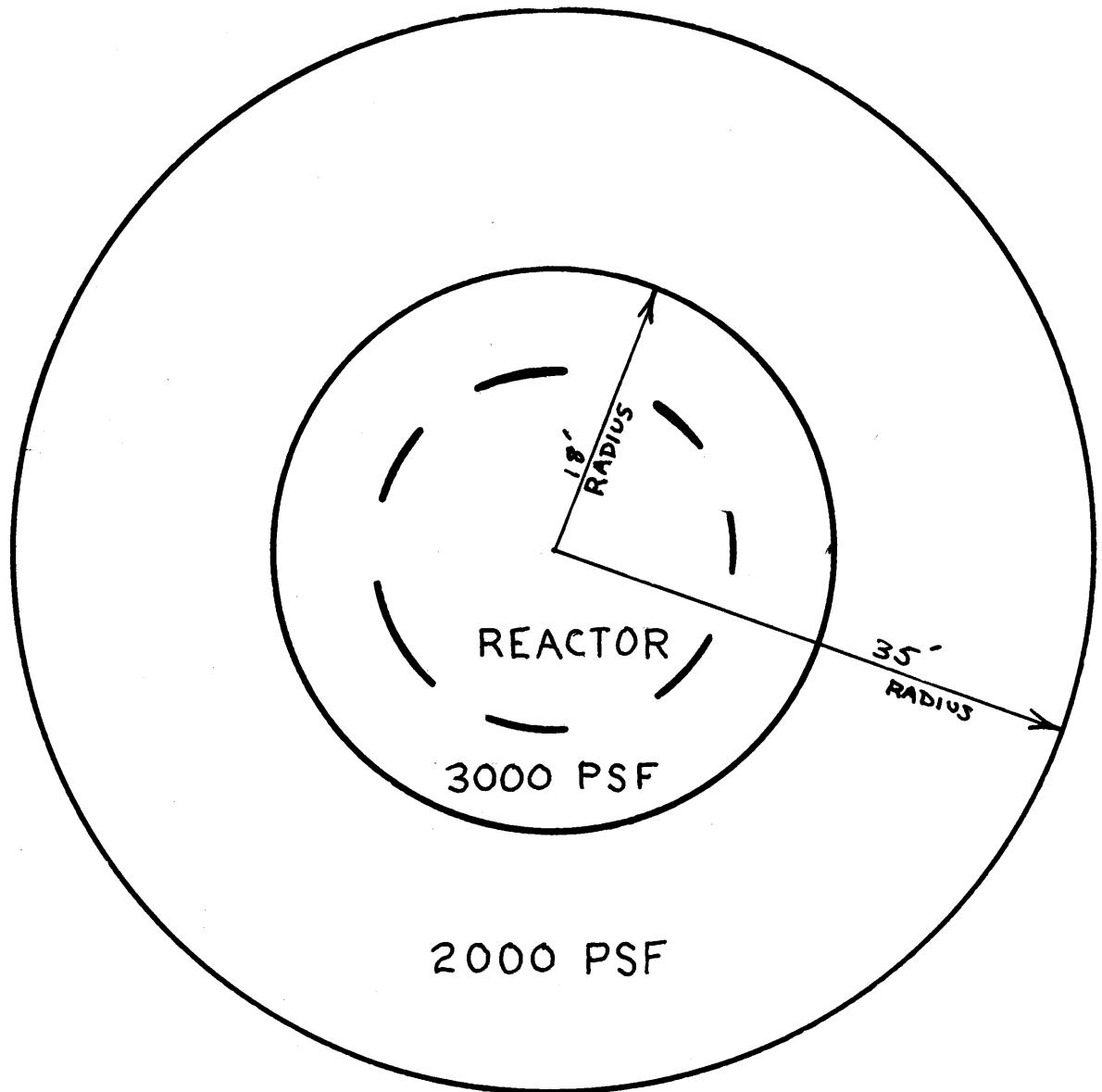
No problems were discovered that would result in a potential reactor hazard for the design of the MITR-II.

3.2 REACTOR FLOOR DESIGN LOADINGS

Referring to Figure 3.1, a six foot ring around the reactor was designed for a live load of 3,000 pounds per square foot; and the balance of the floor was designed for 2,000 pounds per square foot. The total design live load of the floor was 2,000 kips (1 kip = 1,000 pounds) and the lattice facility area of the reactor floor was designed to be fully loaded (F2).

Figure 3.2, shows a simplified representation of the MITR-I lattice facility and the proposed MITR-II lattice facility (the MITR-I lattice facility is decreased in height

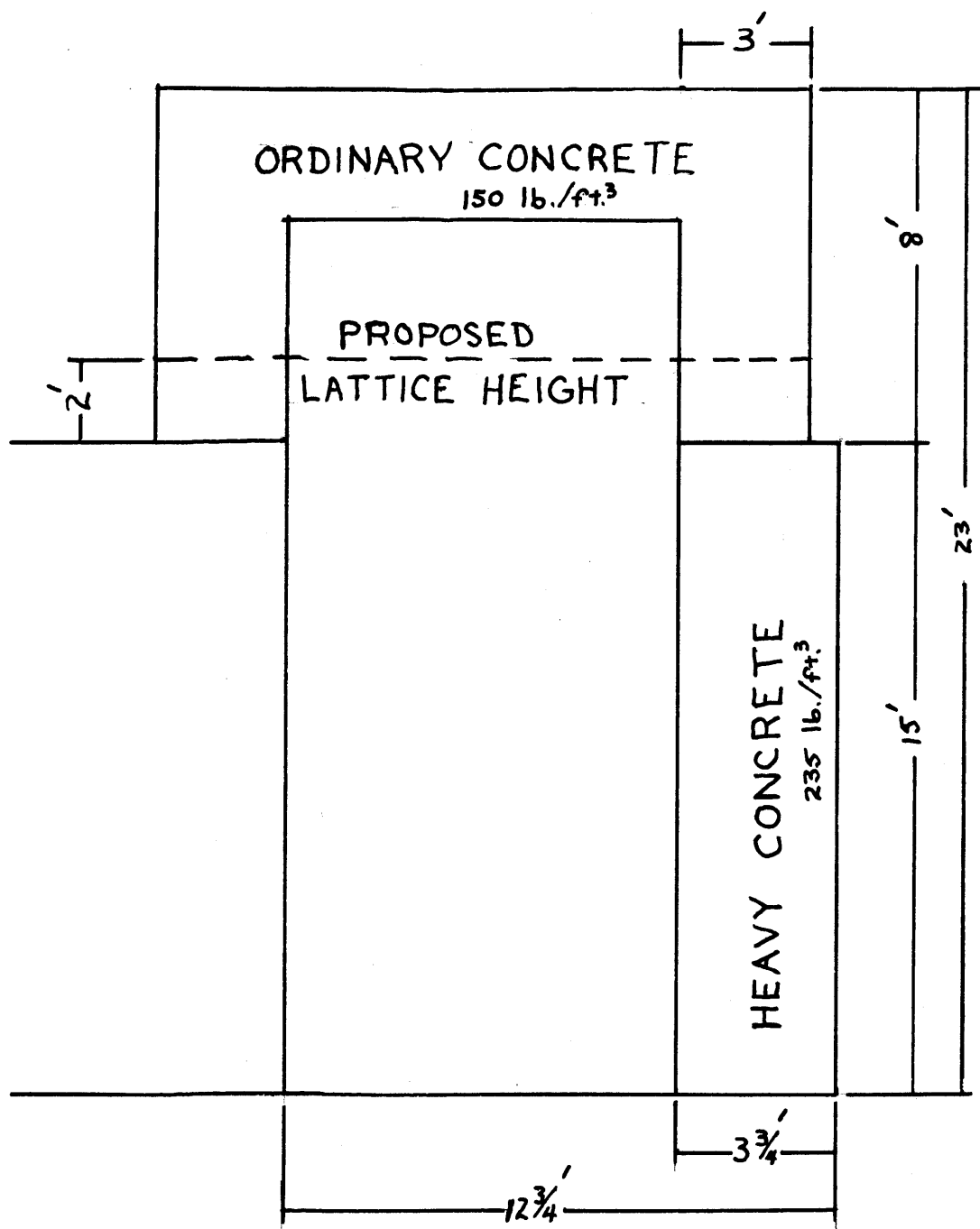
FIGURE 3.1



REACTOR FLOOR DESIGN
LOADINGS

FIGURE 3.2

SIMPLIFIED REPRESENTATION OF LATTICE



by six feet). The maximum local loading and the approximate total load for both the MITR-I and the proposed lattice facility are shown in Table 3.1.

Table 3.1

LATTICE FACILITY LOADS

	Maximum local load (kips)	Approximate total load (kips)
MITR-I Lattice	4.725	700
Proposed Lattice Facility	3.825	550

While the loads due to both structures are well within the total design live loads, and the probability of other areas being fully loaded is very small, both lattice facilities yield local loads above the design 3,000 pound per square foot (psf) within six feet of the reactor and 2,000 psf beyond six feet from the reactor. During construction of the MITR-I lattice facility, careful measurements of the reactor floor were made to determine any deflections of the floor because of the lattice loading. No measurable deflection was found.

While the reactor floor has shown no signs of yielding or deflecting under the MITR-I lattice facility loading (which is not surprising because of the generous conservatism shown in designing the reactor building (F2)), it is

difficult to predict how much more additional loading the floor could safely take in that area, because it is already loaded at about twice its design value. However, for the proposed MITR-II lattice facility, it can obviously be stated that the floor area in the vicinity of the lattice facility will take a 25% increase in load without damage, because the reactor floor had safely supported the MITR-I lattice facility (Load MITR-I Lattice = $(1 + 0.25)$ Load proposed MITR-II Lattice). The proposed lattice floor area will in effect, have been tested for a 0.25 g. vertical acceleration by the experience with the MITR-I lattice. A vertical acceleration of 0.25 is greater than the peak potential vertical acceleration. Horizontal earthquake motions are resisted by steel bands around the lattice facility.

In any event, although failure of the reactor floor in the area of the lattice facility might cause damage to the primary system piping in the equipment room, there would be no damage to the core tank or the core tank supporting structure.

3.3 PIPING

The piping systems in the MITR-II reactor have short period fundamental modes, well above the normal earthquake frequencies. The longest unrestrained run of a major pipe is the light water coolant pipe which runs from the equipment room to the core tank (the pipe is actually restrained

against large motions by the compactness of the area through which it passes). The first fundamental mode of this pipe is 97 cycles per second (Calculation is in Appendix E). Resonance response of the piping appears unlikely.

The need for flexibility in piping to accommodate thermal movement provides sufficient flexibility for differential movements of equipment during earthquake motions. It is recommended that consideration be given to lateral restraints of small piping in the following systems to assure that adequate seismic restraints are provided:

1. Ion Exchange Unit
2. Heavy Water Cleanup System
3. City Water Pipe
4. Helium supply system to D₂O gas holder
5. D₂O Sampling system

With the restraint of the above systems, the piping does not appear to be a major concern because of short runs, numerous restraints, and low pressures.

3.4 SEISMIC EFFECT ON CONTROL RODS

3.4.1 Description of Control Rods Assembly

The control rod assembly is shown in Figure 3.3. The absorber blades travel in slots in the core housing with a nominal 1/16 inch clearance all around. The blade is offset, attached to a magnet armature rod that moves in a slit cylindrical guide tube. Analysis will be made of the in-

crease in rod drop time from seismic motion, rod whip during earthquake motion, and the blade displacement from a lg. lateral acceleration.

3.4.2 Drop Time

In the MITR-II, scram is accomplished by interrupting an electric current to the magnets by which the rods are suspended so that the rods are free to fall in their guide tubes. If these guide tubes can be considered frictionless, lateral forces will be unimportant (lateral forces will be considered in Section 3.4.3). Suppose a scram is initiated during an earthquake that is causing the entire reactor structure to vibrate in the vertical direction with a period on the order of 0.1 or 0.2 seconds and with acceleration varying accordingly ($\pm .1$ g., which is typical of strong-motion earthquakes as recorded by vertical component seismometers) (N1). When the current breaks, the control rod, along with the reactor, will have either upward, downward, or zero velocity with respect to the earth's mass as a whole. Since the magnitude of the vertical ground displacement in typical strong-motion quakes has rarely been known to exceed ± 2 centimeters, the effect of any change in total travel on rod-drop time is insignificant. The effects of initial velocity of the rod at the time the magnet releases may be more significant. Suppose that at release the rod has an upward velocity of 0.3 ft/sec, (N1) which is not unreasonable in

FIGURE 3.3

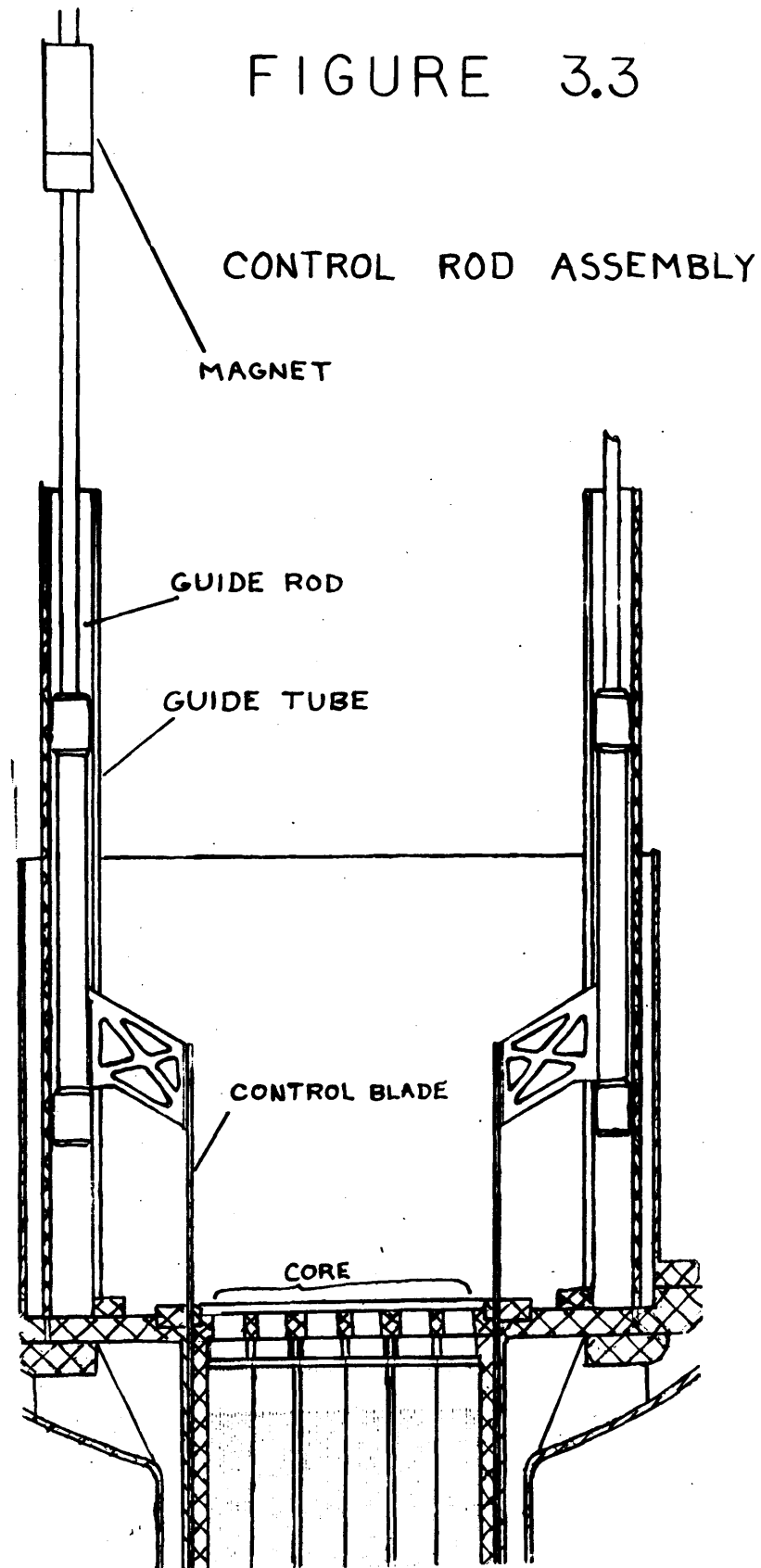
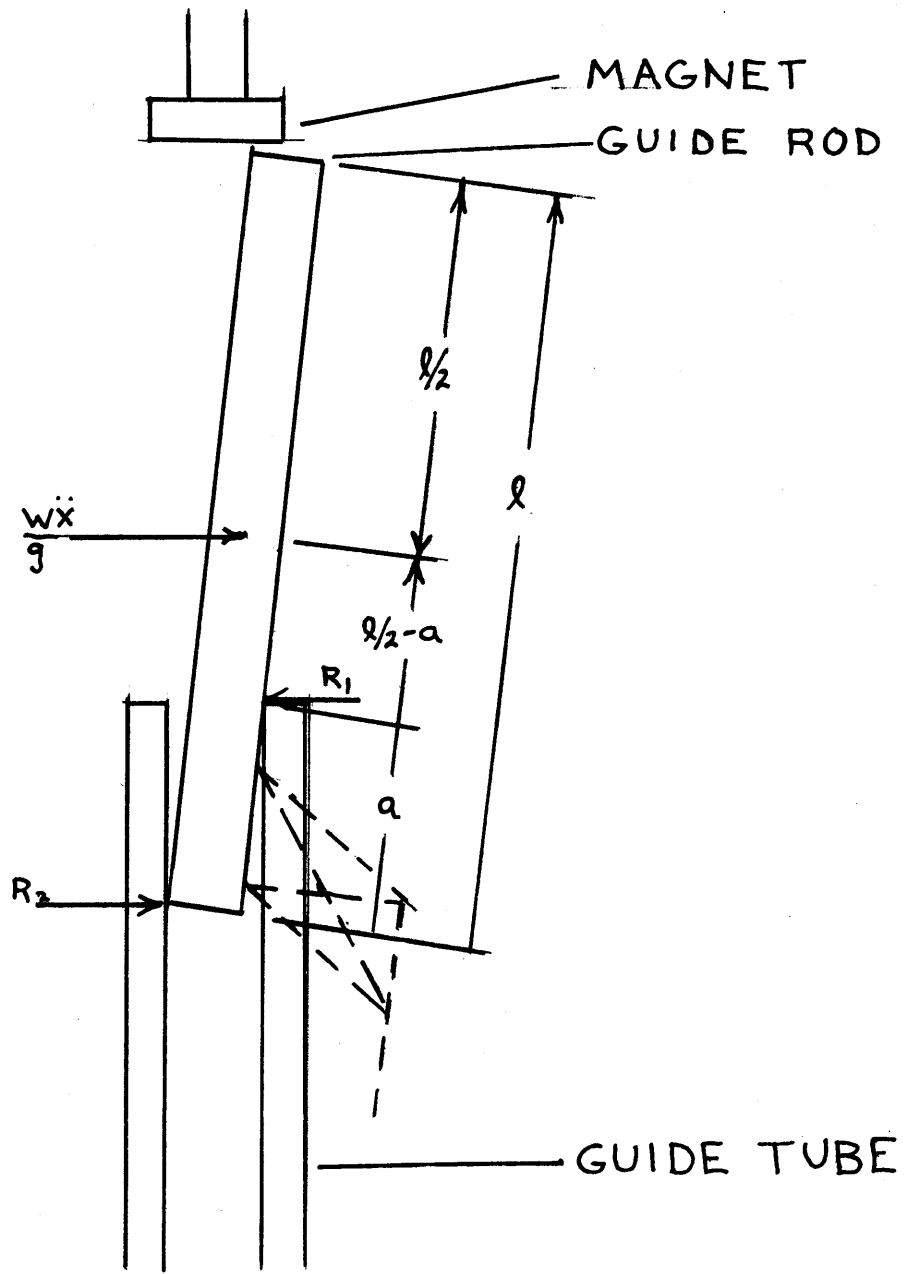


FIGURE 3.4

ROD IN CONTROL ROD GUIDE TUBE



strong quakes. The rod, once free, must continue upward until this velocity is reversed by gravity, which causes a theoretical delay of

$$\frac{2v}{g} = \frac{2(0.3)}{32.2} = 0.02 \text{ seconds} \quad (3.1)$$

Since the individual motions and reversals of the core and control rods imposed by earthquakes are erratic both in time and magnitude, a detailed analysis of all probably sequences of events in this initial split second is probably not meaningful, however, as a worst case assumption, one can assume a delay in the beginning of the free-fall drop cycle on the order of 0.02 seconds. A time delay of 0.02 seconds does not appreciably change the average drop time of 0.68 seconds.

3.4.3 Rod Whip During an Earthquake

Consider the rod in the control rod guide tube as shown in Figure 3.4. Assume that the reactor is being accelerated to the left at a rate g' due to the earthquake, that the rod is rigid, and that its density does not vary along its length.

If the center of mass of the rod is within the guide tube, the effect of lateral acceleration will be to develop small friction forces between the rod and guide. Since the lateral acceleration g' will probably not exceed 10 ft/sec^2 ($\sim 1/3 g$) even in a very strong earthquake, these forces will generally be small, depending on the friction coefficient and the mass of the rod. For instance, in the MITR-II the rod

weighs approximately 25 lbs. Assuming a conservative friction coefficient of 1.0 (01), the retarding friction force will be:

$$\frac{25 \text{ lbs.}}{32.2 \text{ ft/sec}^2} \times 10 \text{ ft/sec}^2 \times 1.0 = 7.8 \text{ lbs.} \quad (3.2)$$

This is not a constant retarding force. Actually, acceleration can reverse direction several times during the rod fall, varying from zero to $\pm 10 \text{ ft/sec}^2$ (assumed maximum, (N1)); thus the rod could rub alternately on opposite sides of the guide tube as it descends.

Considering Figure 3.4 again, a different situation arises if the center of mass of the rod is outside the guide tube. In this case the rod, with the greater fraction of its mass outside the guide tube, will pivot about Z, and resulting reactions at Z and Q can become large due to the lever action of the whipping rod. When the sum of these reactions (R_1 and R_2), multiplied by the coefficient of friction, exceeds the weight of the rod, it will not fall under the influence of gravity. For the MITR-II, the rods are keyed in the guide tube, thus a rotary motion may not develop so that this retarding effect is continuous for the duration of the earthquake.

A condition under which rod jamming could occur is simply derived as follows:

Referring to Figure 3.4:

For acceleration \ddot{x} to the left, the summation of

horizontal forces is

$$R_1 = \frac{w\ddot{x}}{g} + R_2 \quad w = \text{weight of rod} \quad (3.3)$$

The summation of moments about R_1 yields

$$R_2 a = \frac{w\ddot{x}}{g} \left(\frac{l}{2} - a \right) \quad (3.4)$$

or
$$R_2 = \frac{w\ddot{x}}{g} \left(\frac{l}{2a} - 1 \right)$$

Substituting Equation (3.4) into Equation (3.3) yields

$$R_1 = \frac{w\ddot{x}l}{2ag} \quad (3.5)$$

In order for the rod not to jam,

$\mu(R_1 + R_2)$ must be less than w where μ is the coefficient of friction.

Thus

$$\mu \frac{w\ddot{x}}{g} \left[\frac{l}{2a} + \frac{l}{2g} - 1 \right] = \frac{\mu w\ddot{x}}{g} \left[\frac{l}{a} - 1 \right] < w \quad (3.6)$$

or
$$\frac{l}{a} < 1 + \frac{g}{\mu \ddot{x}} \quad (3.7)$$

or
$$\left[1 + \frac{g}{\mu \ddot{x}} \right]^{-1} < \frac{a}{l} \quad (3.8)$$

As an example let

$$g = 32.2 \text{ ft/sec}^2$$

$$\ddot{x} = 10 \text{ ft/sec}^2$$

$$\mu = 1.0$$

then

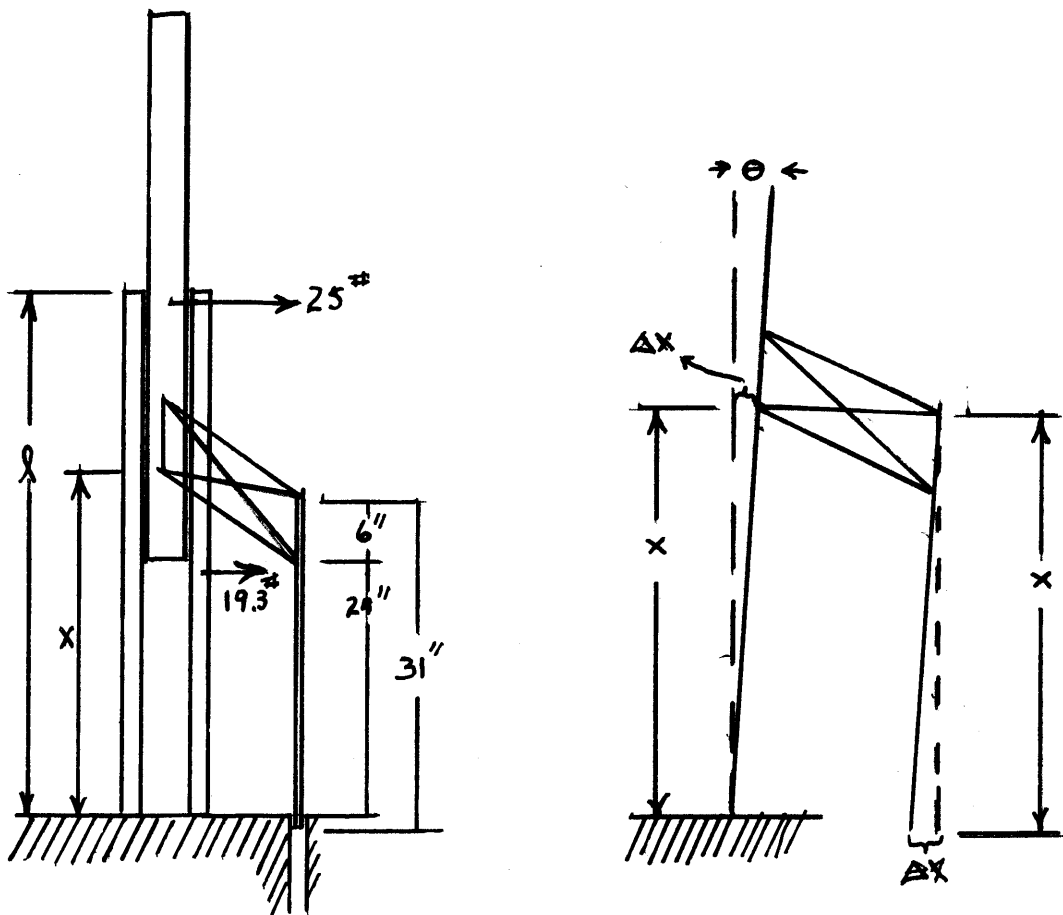
$$\frac{1}{4.22} < \frac{a}{l} \quad (3.9)$$

$$0.238 < \frac{a}{l} \quad (3.10)$$

For the MITR-II, the minimum $a = 23 \frac{1}{8}$ inches and

FIGURE 3.5

MODEL USED TO DETERMINE
CONTROL BLADE DISPLACEMENT



FOR 19 HORIZONTAL

$\ell = 51 \frac{1}{8}$ inches thus

$$\frac{a}{\ell} = \frac{23 \frac{1}{8}}{51 \frac{1}{8}} = 0.45 > 0.238 \quad (3.11)$$

Thus it appears, that for the MITR-II, rod whip will not prevent the rods from dropping during an earthquake.

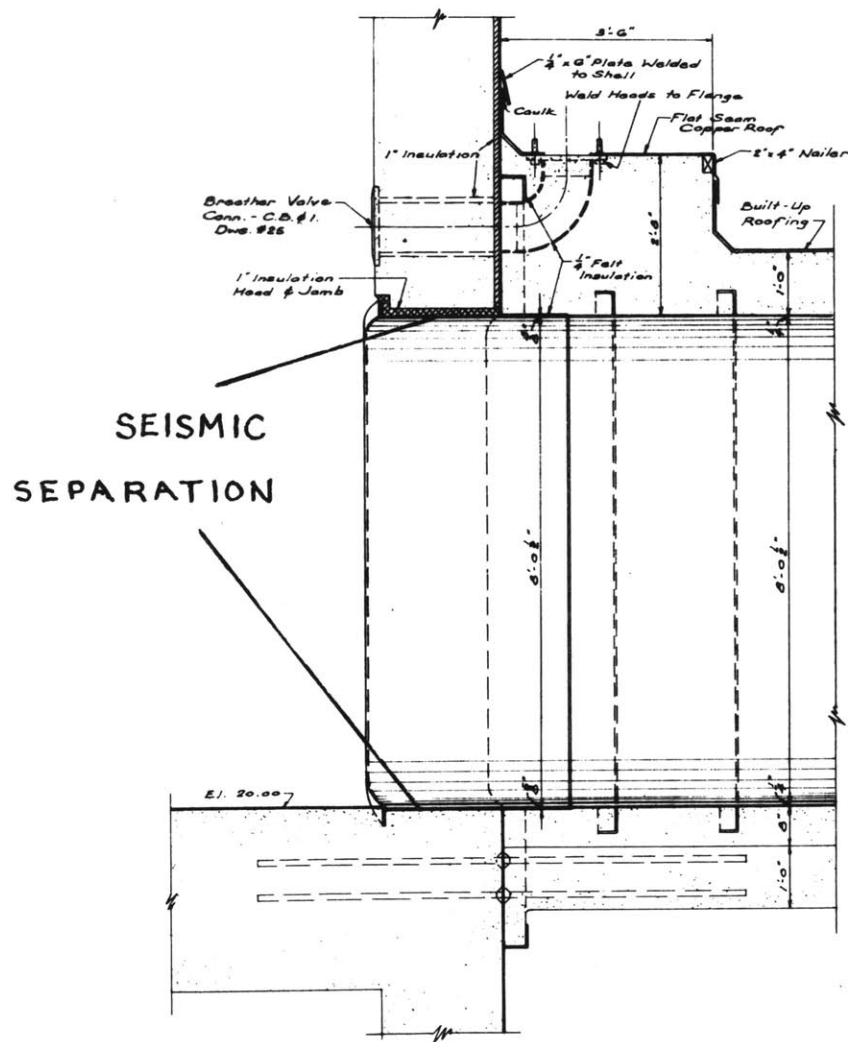
The actual control blades, themselves, cannot whip under earthquake motion because they are constrained at the bottom by their slots, and at the top by the control guide rod. The approximate displacement of the rod guide for a 1g loading was calculated to determine if a large displacement of the control blade might occur which could result in a jammed blade (Calculation is found in Appendix F). The model is shown in Figure 3.5. The displacement Δx , at the end of the blade, shown in Figure 3.5 for a 1 g lateral load was found to be .00634 inches. This is a negligible displacement and according to Mr. Barnett (MITR-II design staff), this will have no effect on rod drop.

3.5 BUILDING PENETRATIONS

Earthquake motion could conceivably cause differential motions between the reactor building and nearby buildings and ground. The reactor building is on a heavily reinforced concrete pad which will shift as a unit as a result of earthquake motion. The reactor building is separated from adjacent structures by a gap in the case of the stack structure and by a felt "seismic" separation in the cases of the entrance air

FIGURE 3.6

SEISMIC SEPARATION OF AIR LOCK



locks and utilities building. Figure 3.6 shows a detail of the seismic separation around the personnel air-lock. The reactor building is able to move independently of the surrounding structures.

Rigid penetrations attached to the reactor building might be broken during an earthquake due to potential differential seismic motions. This problem is particularly acute for below grade penetrations because of lack of freedom of motion of buried pipes. A list of all reactor building penetrations is found in Table 3.2.

The spent fuel pool is entirely below ground water level and breach of the tank would cause leakage of ground water into the spent fuel. It thus appears unlikely that the spent fuel pool would become a radiation hazard before the tank could be repaired.

Special building penetrations for experimental facilities, such as the liquid helium production system and the pneumatic tube sample transfer system, are made in a manner to prevent any radioactivity release. These penetrations can be sealed by automatic isolation valves and by manual operational valves that can be closed from outside the reactor penetrations (S1).

The emergency core spray is to be supplied by two redundant systems connected to city water. The connection to city water in the utilities room is to be by a flexible pipe

Table 3.2

LIST OF PENETRATIONS

<u>Below Grade</u>	
<u>No. of Penetrations</u>	<u>Description</u>
3	4" capped pipe sleeves
1	1 1/4" water effluent pipe from sump
2	10" pipe lines - secondary coolant system
1	30" air effluent duct
1	spent fuel pool
1	2" electric pipe to base of stack
1	Basement personnel lock 3' x 7' door
1	1 1/2" pipe sleeves for pneumatic tubes
3	1 1/2" spare pipe sleeves (capped)
3	4" conduits for gas and electric utilities to equipment room
1	2 1/2" pipe for building pressure relief system
<u>Above Grade</u>	
<u>No. of Penetrations</u>	<u>Description</u>
1	4" sleeve at chopper window
1	24" chopper window
1	1/4" pipe over basement lock
1	2" pipe air conditioning effluent
2	2" pipe air conditioning coolants
1	30" inlet air duct

Table 3.2
(Continued)

1	1" cold water supply	
2	2" pressure test lines	
1	1" pressure test line	
2	10" vacuum breaker lines	
1	1" pipe	
1	2" pipe	
1	3" pipe	gaseous helium lines
1	4" pipe	

Electric Service

No. of Penetrations

3	3" conduit power wiring
1	1" conduit
1	2" C
1	2 ½" C
1	4" pipe
2	1 ¼" C for telephone
3	3/4" C for control wiring

to allow for relative building motions.

If the pipes leading to the waste storage tanks (or the tanks themselves) are damaged by an earthquake, there is a potential leak of radioactive material into the groundwater. It is not intended that the waste storage tanks will be used for highly active waste (S1). In the past twelve years, the sampling prior to discharge has shown that the solutions discharged from the waste tanks has not required extra in-tank dilution prior to discharge into the sewer system with final ocean discharge. Accidental release of this material into the ground water is not predicted to create an off-site concentration above permissible limits in occupied areas.

Although rupturing of any rigid reactor building penetration due to potential differential earthquake motions will not simultaneously cause a major release of activity, the broken penetrations might cause a possible breach in the reactor containment. If an internal D_2O pipe were to be broken at the same time as the breach in the containment, there would be a potential release of tritium by evaporation. Calculations have been made in the MITR-II Safety Analysis Report (S1) which indicate that in the event of a rupture of both the D_2O system and the containment system, the off-site exposure to tritium activity would remain below permissible yearly averaged limits for at least two days. Thus, there would be ample time to evaluate the situation and take

appropriate action.

3.6 SEISMIC INSTRUMENTATION

For a 14-day period from April 1, 1971 to April 14, 1971, a Schaevitz 1 g accelerometer was attached to the reactor building to measure expected everyday building accelerations. The accelerometer was attached to the reactor building shield wall nearest the reactor stack at a position about two feet above the reactor floor level. The electronics of the accelerometer setup used are shown in Figure 3.7 and the accelerometer was calibrated using the force of gravity. The accelerometer was oriented for five days in an approximate north-south direction (normal to the wall) and for five days in an east-west direction (parallel to the wall). For the remaining four days, the accelerometer was used to measure a vertical component of the acceleration.

The MITR-II site is located in an industrialized section of Cambridge, Massachusetts. The site is also adjacent to a railroad right of way. Numerous ground motions result from passing trucks and trains. The accelerometer measured a peak acceleration of these motions and not their frequency. The plot of peak accelerations was less erratic during weekends when the reactor was shut down.

The peak acceleration measured during the 14-day period occurred when the accelerometer was aligned parallel to the shield wall and a train passed on the tracks adjacent to the

FIGURE 3.7

ACCELEROMETER SIGNAL CIRCUIT

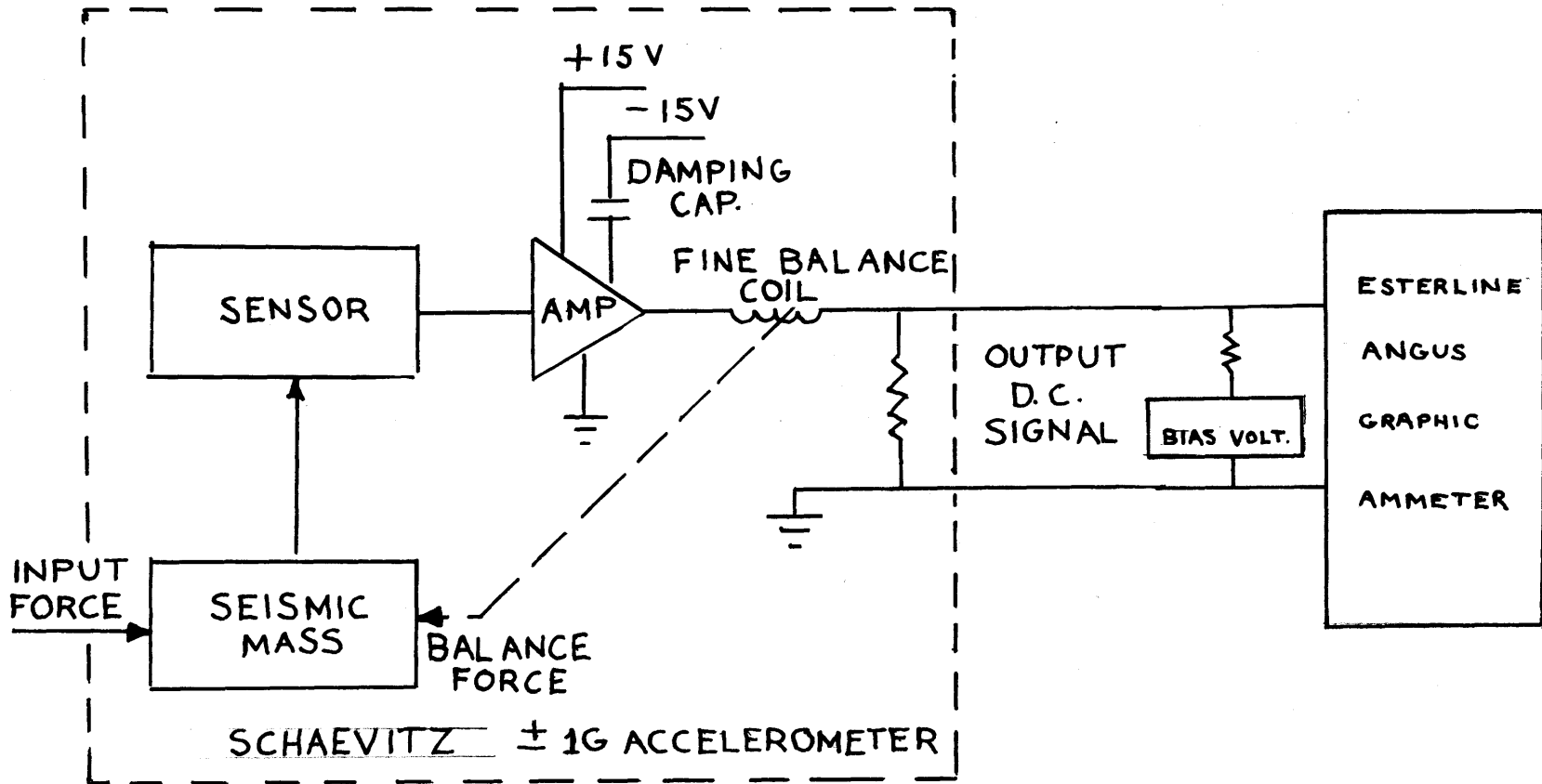
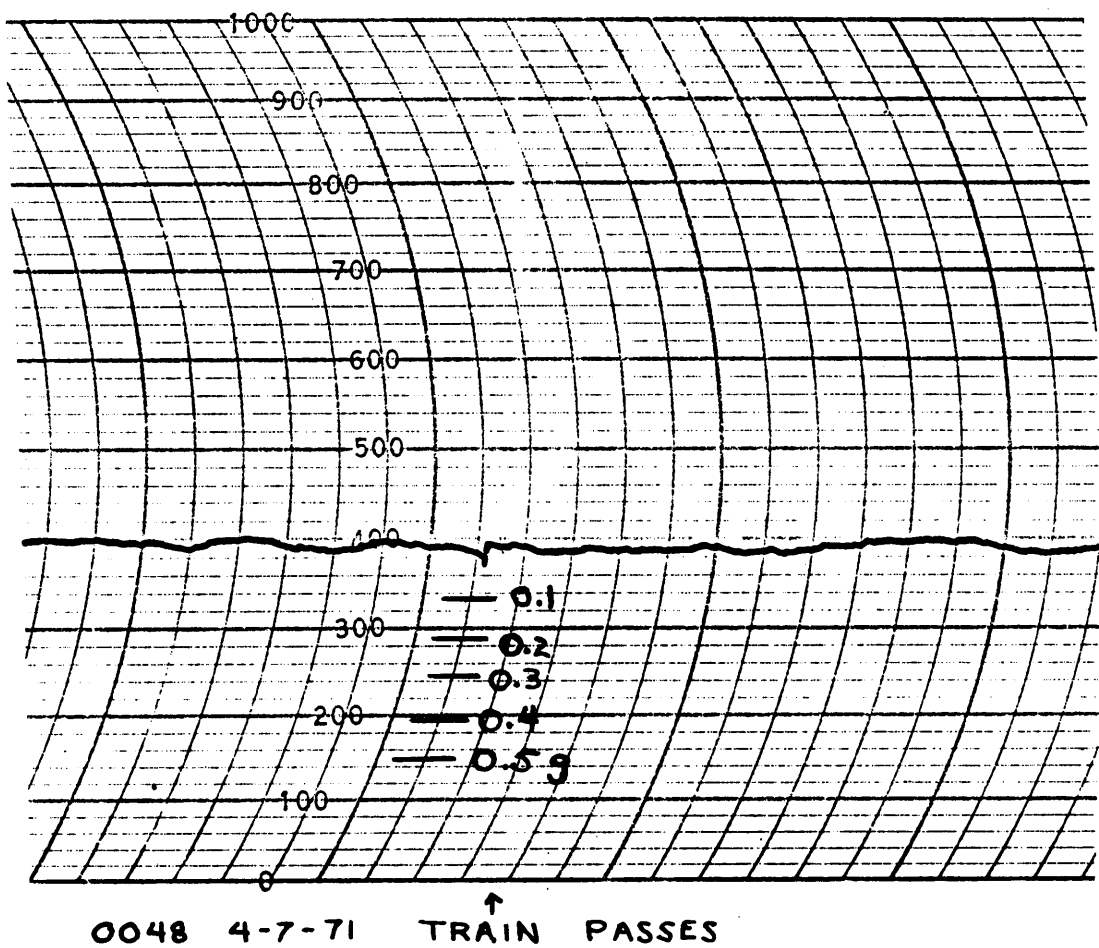


FIGURE 3.8
SAMPLE ACCELEROMETER OUTPUT



site. The accelerometer output for this occurrence is shown in Figure 3.8. This peak acceleration corresponds to about a 0.03 g horizontal acceleration. The reactor operator also noted fluctuations in various galvanometer needles during the passing train.

There are numerous commercial strong motion accelerographs and seismic triggers available with actuating accelerations between 0.005 g to 0.05 g. Because of the numerous industrially related ground motions at the MITR-II site, any proposed seismic trigger should actuate at between 0.04 g to 0.05 g in order to minimize any false "seismic" alarms. Because of major interest in the safety of the core tank, an optimal location of any seismic instrumentation would be on the core tank support structure.

While seismic instrumentation would give the reactor operators the best analysis of building motions, the intensity of the following phenomena will also give the reactor operator a feeling for the extent of earthquake motions:

1. Fluctuation of galvanometer needles
2. Swaying of overhead lights
3. Shaking of equipment
4. Movement of floor

3.7 TEMPORARY SHIELD WALLS

Temporary shield walls of numerous unbonded concrete or lead bricks might fail during earthquake motion. Consequently

temporary shield walls should not be used in the MITR-II where their failure will result in an unacceptable offsite release of radioactivity or where the temporary shield failure could damage important reactor control mechanisms.

Chapter 4

REACTOR STACK

4.1 INTRODUCTION

The 150' reactor stack, which is adjacent to the reactor building, is a possible area of concern in the event of an earthquake. The stack is of the unlined brick variety. As shown by Figure 4.1 of the reactor site, assuming that an earthquake has an equal probability of occurring from any direction, the probability that the stack will fall into zone II, ie., hit the reactor containment, is about .25. (Note: this assumes the primary mode of failure shown in Figure 4.1 as being the worst case, since in higher modes of failure, no material would drop too far from the original vertical position)

4.2 APPROXIMATE EARTHQUAKE ANALYSIS OF STACK

An approximate method of determining the dynamic earthquake shear at various horizontal sections of the stack is to consider the Recommended Lateral Force Requirements (1959) of the Structural Engineers Association of California (SEAOC). The procedure specified is based on only the first mode of the structure, which was assumed to be the failure mode of most concern for the stack. By assuming a characteristic shape for the first mode, it is possible to convert the maximum condition of response into a set of equivalent static forces. The actual analysis may then be

executed on the basis of static analysis (B1).

The basic concept of the SEAOC recommendation is contained in the two formulas

$$V = KCW \quad (4.1)$$

$$C = \frac{0.05}{T^{1/3}} \quad (4.2)$$

where V = dynamic shear at base,
 W = total weight of building,
 T = natural period of first mode,
 K = coefficient reflecting the ability of the structure to deform into the plastic range (= 1.5 for brittle structures).

A computer program was written to calculate T and W for the stack. The program performs the above calculation to determine the dynamic shear and adds the effect of a 100 MPH wind (22 lb/sq.ft. of Frontal Area) in the same direction as the dynamic shear. The program then calculates the shear stress at 25 different heights of the stack and, because of the stack's circular cross section, the shear stress recorded is increased by 50%. A listing of the program is included in Appendix G.

The period of the fundamental mode was 1.7 seconds. The calculated results are shown in Table 4.1. Allowable shear stresses for brick stack are given by the formula (M3)

$$f_{\text{psi}} = 12.3 + 0.037h \quad (4.3)$$

h = height from top
 (assumes allowable shear stress = 2/3
 allowable working tension)

The allowable stresses are included with the calculated stresses in Table 4.1 and in all cases the calculated stresses

Table 4.1

SHEAR STRESSES IN STACK FROM 100 MPH WIND
AND SEACO DESIGN CODE DYNAMIC SHEAR

Total DYNAMIC SHEAR at Base = 36,586 # (+SEACO)

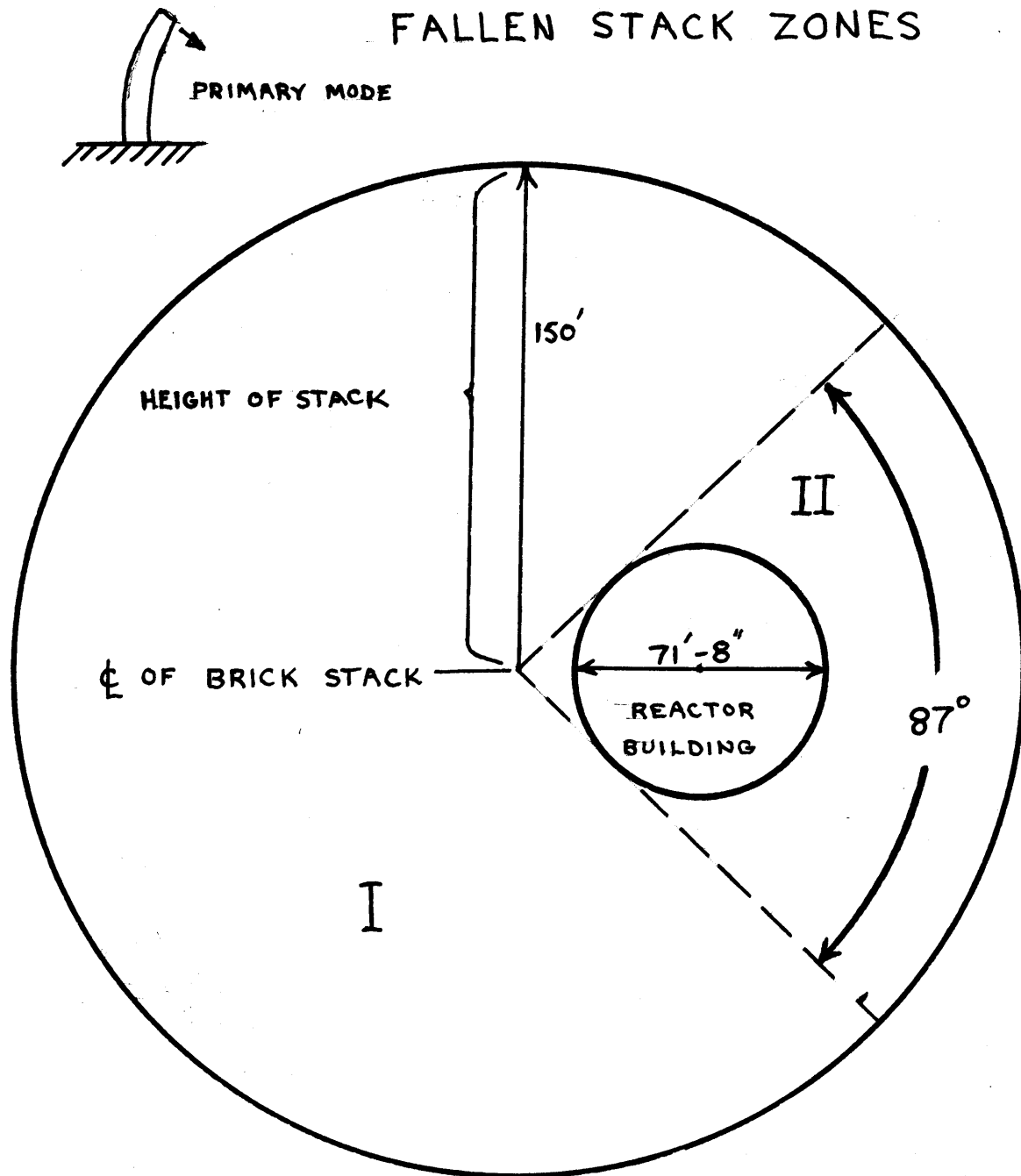
Section	Total Shear in psi Wind and SEACO	Height from Top h	Allowable Shear Stress* $f=12.3 + 0.037h$ (reference M3)
1	2.39	6	12.5
2	4.21	12	12.7
3	5.73	18	13.0
4	7.01	24	13.2
5	8.10	30	13.4
6	9.03	36	13.6
7	9.84	42	13.8
8	10.53	48	14.0
9	11.13	54	14.2
10	11.64	60	14.4
11	12.08	66	14.7
12	12.44	72	15.0
13	12.74	78	15.2
14	12.97	84	15.4
15	13.15	90	15.6
16	13.28	96	15.8
17	13.35	102	16.1

Table 4.1 Continued

18	13.37	108	16.3
19	13.35	114	16.5
20	13.28	120	16.7
21	13.17	126	16.9
22	13.01	132	17.2
23	12.81	138	17.4
24	12.57	144	17.6
25	12.29	150	17.8

* Assumes Allowable Shear Stress = $\frac{2}{3}$ Allowable Working
Tension of Brickwork

FIGURE 4.1



- I REACTOR BUILDING IS NOT HIT BY STACK
 II REACTOR BUILDING IS HIT BY STACK

are less than the allowable stresses.

4.3 WORST CASE OF STACK FAILURE

In the event that the stack were to collapse, a calculation has been made in which the assumed worst case of stack failure was modeled, and the resultant stresses of the containment building shell roof from the fallen stack were calculated by using the SABOR-5 program.

4.3.1 Load Model

The loading model is shown in Figure 4.2. The stack is assumed to be hinged at the base and allowed to fall toward the containment building. Once leaning over the containment building, the stack falls in sections onto the containment building. Section N of the stack results in a load in zone N on the containment. Zones on the containment building are determined by the "shadow" of the stack on the containment building. The mass of stack sections ① and ② are doubled to take into account the effect of impact. The mass of the stack below 39 feet is not included in the analysis because it cannot hit the containment roof and it could only hit the rigid shield wall.

The loads used in each zone are shown in Table 4.2. The weight of the roof is also used in the stress calculation. The maximum local loading corresponds to about 5.4 psi.

4.3.2 Calculational Model

The containment building roof was divided into 23

Table 4.2

LOADS USED IN FALLEN STACK PROBLEM

Zone Section Struck by Mass of Stack	Equivalent Mass of Stack Hitting Sec- tion (increased because of im- pact)	Area Struck	Equivalent Load in psi
1 and 2	113,700#	160 sq/ft	5.0 psi
3	37,900#	90 sq/ft	3.0 psi
4	64,900#	104 sq/ft	4.3 psi
5	69,200#	112 sq/ft	4.3 psi
6	90,000#	119 sq/ft	5.25 psi

Weight of Roof	Element	13 use .114 psi
	Element	13 use .158 psi

FIGURE 4.2

MODEL OF FALLEN STACK

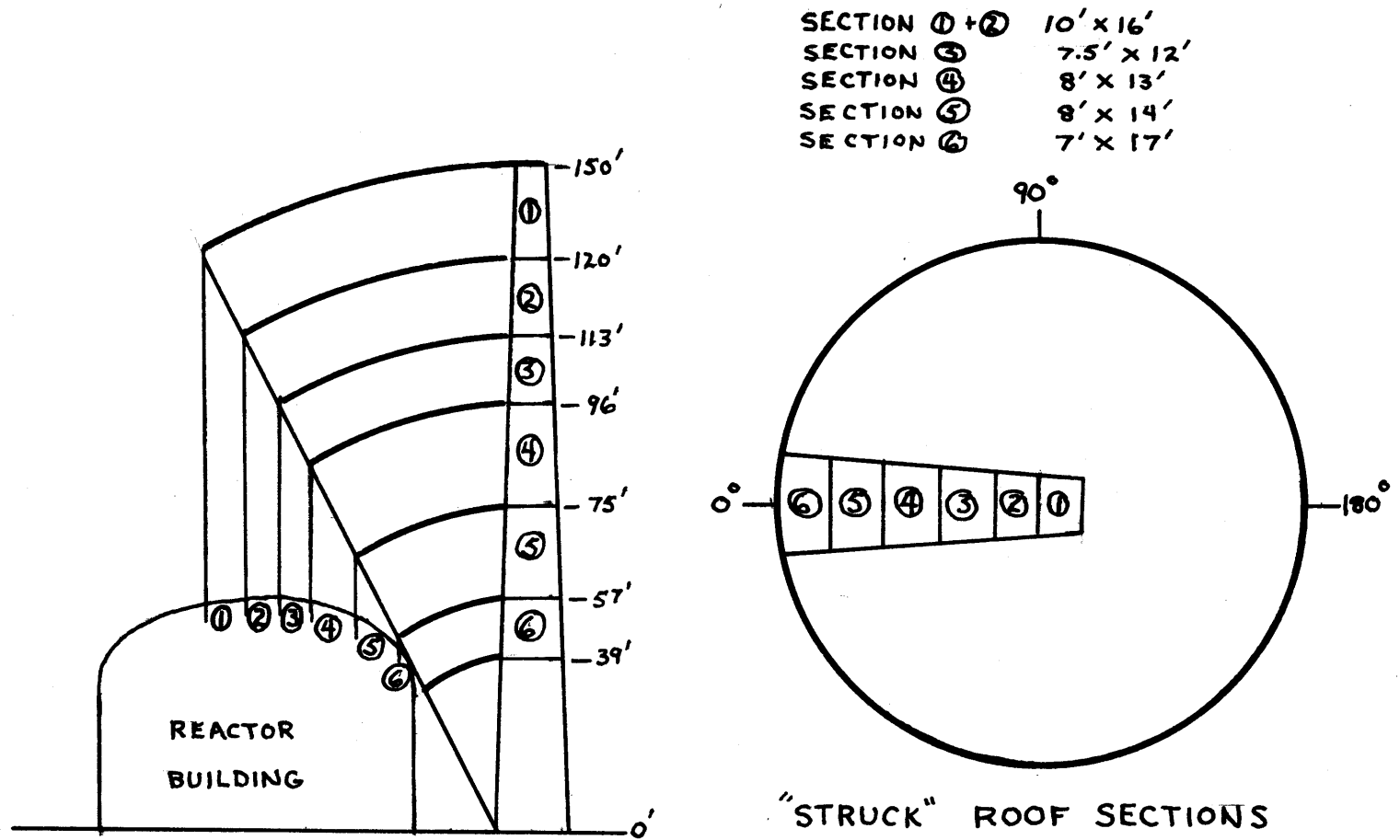
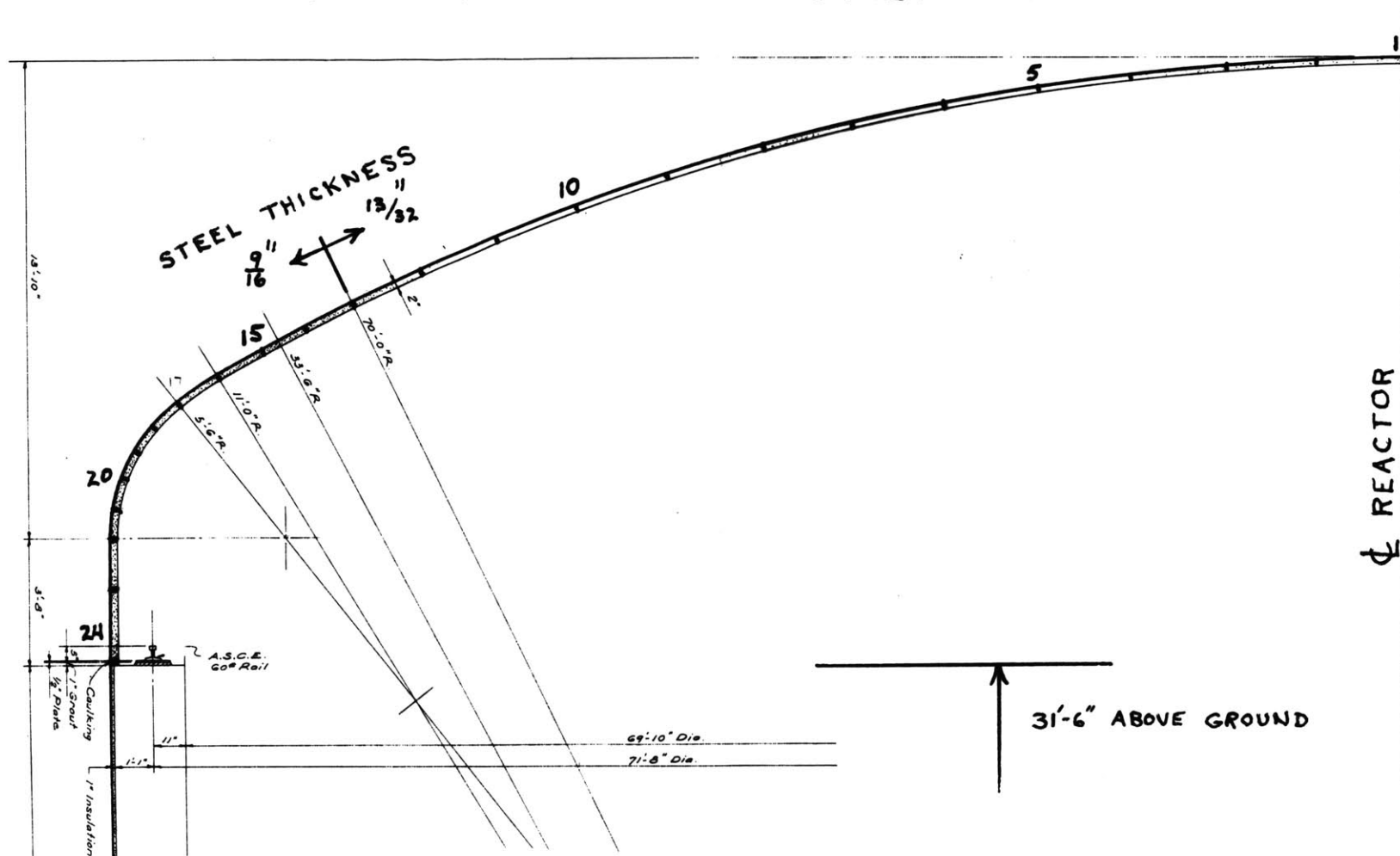


FIGURE 4.3

ELEMENT DIVISIONS OF CONTAINMENT ROOF



discrete elements as shown in Figure 4.3. Node 24 (corresponding to the top of the concrete shield wall) was considered to be a fixed point. The discrete zone loads were applied to the containment building by using the fourier harmonics 0, 1A, 1B, 2A, 2B, 3A, 3B, 4A, 4B, 5A, 6A, 7A, and 8A. The harmonic loading gave loads within 5% of the actual discrete unaxisymmetric loads.

4.3.3 Local Buckling of Roof

The critical pressure (P_{cr}) of local buckling of a spherical shell is given by the equation: (B3)

$$P_{cr} = 0.365 E (t/R)^2 \quad (4.4)$$

For our case Roof thickness = $t = 13/32$ (inches)

Shell radius of curvature = $R = 840$ (inches)

Modulus of elasticity = $E = .3 \times 10^8$ (psi)

This yields a critical pressure of local buckling:

$$P_{cr} = 2.5 \text{ psi} \quad (4.5)$$

Since the fallen stack loading results in equivalent pressure loads of around 5 psi, it appears that the roof will undergo local buckling from the fallen stack.

4.3.4 Results of SABOR-5 analysis

The peak stresses on the containment building roof from the fallen stack are given in Table 4.3. These stresses occur on the inside surface of the containment roof. The peak stresses correspond to about one third of the yield point (33,000 psi) and about one fifth of the ultimate strength (60,000 to 72,000 psi) of the A-283-C steel

Table 4.3

STRESSES ON CONTAINMENT FROM FALLEN STACK LOADING OF SABOR-5

Circumferential Station	0°		90°		180°	
Element	(psi)	(psi)	(psi)	(psi)	(psi)	(psi)
Station 2 Inner Surface	11,161	8,592	2,947	6,941	9,925	8,560
Station 4 Inner Surface	12,638	1,034	4,181	406	11,698	838
Station 8 Inner Surface	12,982	3,192	1,243	308	824	434
Station 16 Inner Surface	7,404	1,262	195	248	301	206
Station 20 Inner Surface	3,402	494	990	30	817	8

plate (M2).

Thus SABOR-5 stress levels indicate that the containment roof will not fracture under the fallen stack loading (this may not hold true if the temperature of the steel is below the ductile transition temperature of 0° F (M2), which is highly unlikely since the building is always heated). Thus it seems that although the shell may buckle under the falling stack, that it is unlikely that the roof will be fractured. The 20 ton polar crane which is supported on thick concrete shield walls should provide a more than adequate means of limiting the buckling of the roof. It appears therefore highly improbable that any significant parts of the stack would be able to penetrate through the reactor shielding and cause any damage to the reactor core tank. Although the containment system might no longer be leakproof, the effect of the earthquake will not simultaneously cause a problem in the reactor core for which the containment would be required.

4.4 SUMMARY

While there is some probability of the stack hitting the containment (~25%) if it fails, it appears that even though the containment building may buckle locally, it will not be penetrated by a significant portion of the fallen stack. In addition, using the SEAOC design and the allowable shear stress for brick stacks, it appears that the

dynamic stress will not be sufficient to cause failure of the stack.

According to Mr. J. Fruchtbaum (Office of J. Fruchtbaum, Buffalo, New York), who set the design specifications for the stack, special precautions were taken to make the stack very stable; and Mr. Lohr, who was in charge of the construction of the stack, stated that perforated brick was used with liberal amounts of mortar in the joints.

Chapter 5

SUMMARY

The peak potential horizontal acceleration expected at the MITR-II site is approximately 0.2 g. The MITR-II core can be adequately cooled and shutdown so that no major radioactivity release will occur, provided that the core tank remains intact. Analysis of the reactor core tank indicates that much higher accelerations than 0.2 g are necessary to cause failure of the core tank. There does not appear to be any significant resonance effect between earthquake motions and the core tank structure or the main coolant pipes, but in any case, it would take a horizontal acceleration of 5.1 g combined with a vertical acceleration of 3.4 g before the peak stress of the core tank would equal the yield stress of aluminum. These stresses are far higher than any predictable effect of an earthquake.

While it is conceivable that the effect of an earthquake might cause some damage to the reactor stack, it has been calculated as shown in Section 4.2, that it is highly unlikely that peak seismic shear stresses would be above the allowable shear stress of brickwork. It is recommended that the reactor stack be inspected on a regular basis to insure that there has been no deterioration of mortar or brickwork. This inspection process will add assurance that the stack will be able to withstand earthquake motions.

During construction of MITR-II, checks should be made that there is adequate lateral restraint of all piping systems. Future penetrations in the reactor building should be made flexible enough to allow for differential earthquake motions.

Temporary shield block walls should not be located where their failure might cause major equipment damage or radioactive release.

Within the scope of this report, it appears that the design MITR-II is adequate to provide required protection even in the event of the maximum expected earthquake motions.

Appendix A

SABOR-5 RESULTS OF THE REACTOR VESSEL

Table A.1 Static Case Comparison of Calculations

Table A.2 Comparison of Static Sabor-5 Case with Free-body Diagram

Figure A.1 Free-body Diagram of Core Tank

Table A.3 Inner Vessel Stress

Table A.4 Outer Vessel Stress

Table A.1

STATIC CASE COMPARISON OF CALCULATIONS
(operating condition without D₂O reflector)

Method	Peak Stress at Bottom of Core Tank
Hand Calculation Ref. ASME Code for Pressure Vessels, Section VIII	1125 psi
SABOR-5 Program Computer Calculation	1426 psi

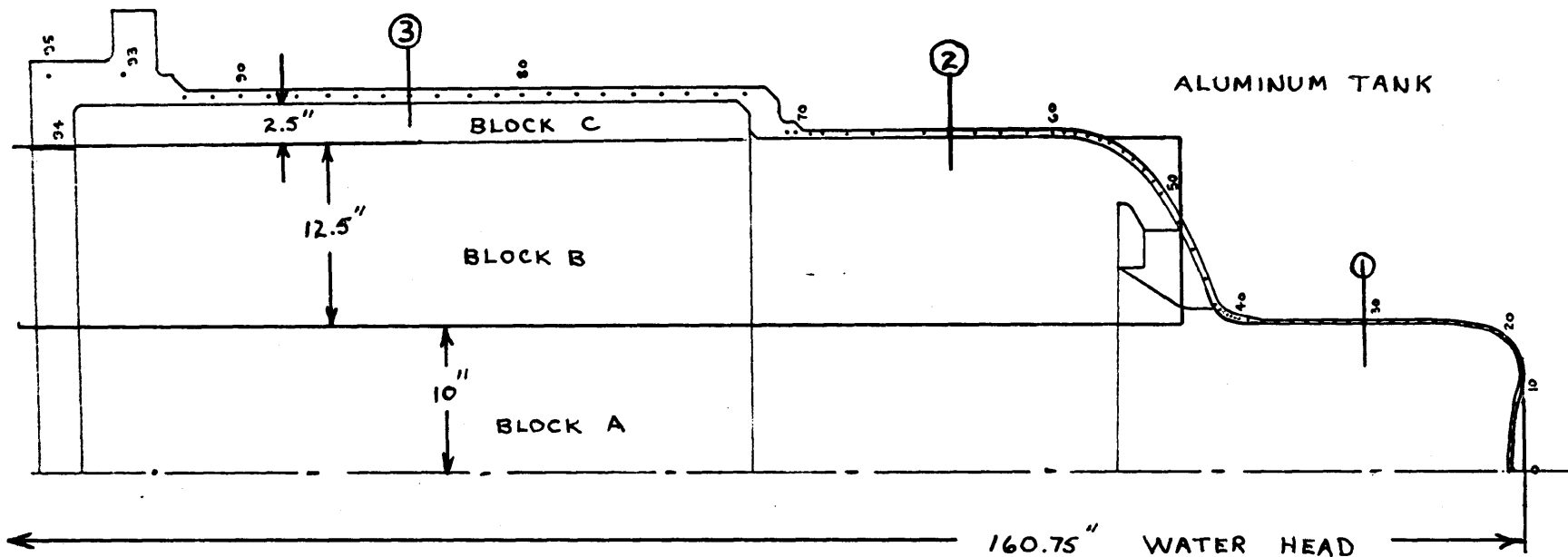
Table A.2

COMPARISON OF STATIC SABOR-5 CASE WITH
FREE BODY DIAGRAM

(Hand Calculation Ref. 15.A-3)

Location of Station	Approximate Stress From Free Body Diagram	σ _s From Static Case of SABOR-5
Station 31	116 psi	116.8 psi
Station 64	141 psi	168 psi
Station 84	83 psi	93 psi

FIGURE A.1
CORE TANK FREE-BODY DIAGRAM



INCLUDING INTERNAL STRUCTURE*

MASS BLOCK A = 1820 # (POUNDS)

MASS BLOCK B = 8270 #

MASS BLOCK C = 3160 #

* ADDS 2397 # TO B

SECTION	CROSS SECTIONAL AREA	STRESS
①	15.7 SQ. INCHES	116 PSI
②	71.5 SQ. INCHES	141 PSI
③	160.0 SQ. INCHES	83 PSI

Table A.3

INNER VESSEL STRESS

(Flow Shroud)

Loading Condition

Static + $\frac{1}{2}$ G sideways + 1/3 up

	Peak σ_s (psi)	Peak σ_o (psi)	Peak σ_{so} (shear)
0°	47	55	165
45°	36	47	142
90°	.7	38	88
135°	-18	-20	19
180°	-25	-3.6	0

Station 37	Station 40	Station 79
---------------	---------------	---------------

 σ_s = linear surface stress (perpendicular to σ_o) σ_o = hoop stress σ_{so} = shear stress

Table A.4

OUTER VESSEL CRITICAL AREAS

G	Outer Core Tank Bottom				Outer Core Tank Support Area for Inner Vessel (feet area)				
	Peak σ_s (psi)	Station	Peak σ_e (psi)	Station	Leg Area Peak σ_s (psi)	Station	Leg Area Peak σ_e (psi)	Station	
0	0°	1333	16 inner layer	1426	11 outer layer	1753	50 inner layer	791	48 outer layer
0.5	0°	1766	16 inner	1900	11 outer layer	2590	50 inner layer	814	48 outer layer
0.33	90°	1764	16 inner	1897	11 outer	2020	50 inner	868	48 outer
	180°	1763	16 inner	1896	11 outer	1885	50 inner	907	48 outer
1.5	0°	2628	16 inner	2846	11 outer	4036	50 inner	1113	48 outer
	90°	2623	16 inner	2836	11 outer	2984	50 inner	1288	48 outer
1.0	180°	2619	16 inner	2835	11 outer	2744	50 inner	1405	48 outer
4.5	0°	5225	16 inner	5693	11 outer	8589	50 inner	2121	48 outer
	90°	5209	16 inner	5667	11 outer	5995	50 inner	2637	48 outer
3.0	180°	5196	16 inner	5657	11 outer	5295	50 inner	2973	48 outer

Appendix B

Fortran IV Computer Loads Program used to generate loading input to SABOR-5 for the inner flow shroud.

```

C *****
C
C PROGRAM TO CALCULATE INNER VESSEL LOADS
C
C THERE ARE SIX LOADS ASSOCIATED WITH EACH ELEMENT AND THEY ARE
C DENOTED BY
C F1,F2,....,F6 AND THEY REPRESENT
C
C F1=AXIAL LOAD AT S=0
C F2=CIRCUMFERENTIAL LOAD AT S=0
C F3=NORMAL LOAD AT S=0
C F4=AXIAL LOAD AT S=L
C F5=CIRCUMFERENTIAL LOAD AT S=L
C F6=NORMAL LOAD AT S=L
C
C LOADS FOR 4 HARMONICS FOR EACH OF 3 LOADING CONDITIONS ARE
C GENERATED. I.E. FOR GSIDE=0,5,2,5,4,5
C
C *****
C DIMENSION X(100),PHX(100,2),T(100,2),R(100,2),Y(100),Z(100,2),
C IPHI(100,2),TIT(20),NX(4),A(9)
C DENSITY OF WATER
C RHOW=7.03613
C DENSITY OF ALUMINUM
C RHOA=0.1
C NUMBER OF NODES
C NODES=80
C NUMBER OF ELEMENTS
C NEL=79
C NI=1
C READ AND DEFINE THE GEOMETRY
C READ (4,1000) (X(I),Y(I),I=1,NODES)
C DO 100 I=1,79
C Z(I,1)=X(I)
C Z(I,2)=X(I+1)
C R(I,1)=Y(I)
100 R(I,2)=Y(I+1)
1000 FORMAT (2E12.6)
C READ (4,1001) (PHX(I,1),PHX(I,2),I=1,NEL)
C DO 101 I=1,NEL
C PHI(I,1)=PHX(I,1)*0.0174533
101 PHI(I,2)=PHX(I,2)*0.0174533
C DO 102 I=1,3
C T(I,1)=1.5
102 T(I,2)=1.5
C T(4,1)=1.5
C T(4,2)=2.5625
C T(5,1)=2.5
C T(5,2)=1.625
C T(6,1)=1.625
C T(6,2)=1.625
C T(7,1)=1.625
C T(7,2)=0.8
C DO 103 I=8,79
C T(I,1)=0.75
103 T(I,2)=0.75
1002 READ (4,1002) E1,E2,E3,E4,E5
1002 FORMAT (3X,5E12.6)
1001 FORMAT (8X,2E12.6)
C NZERO=0
C NSABOR=10
C NHARM=4
C START PUTTING OUT THE SABORS DATA CONTROL CARDS

```

```

      NONE=1
      DO 950 IKL=1,3
      WRITE (7,1003) NZERO,NEL,NODES,NZERO,NHARM,NZERO,NZERO,N1,NSABOR,
1NZERO,N1
1003 FORMAT (11I4)
      WRITE (6,1004)
1004 FORMAT (' LANCE TITLE?')
      READ (5,1005) (TIT(I),I=1,20)
1005 FORMAT (20A4)

      WRITE (7,1005) (TIT(I),I=1,20)
      WRITE (7,1003) NZERO
      ZERO=0.0
      WRITE (7,1007) (X(I),Y(I),I=1,NODES)
      DO 104 I=1,NEL
      J=I+1
      WRITE (7,1006) I,J,PHX(I,1),PHX(I,2)
1006 FORMAT (2I4,2E12.5)
      104 CONTINUE
1007 FORMAT (2E12.5)
      N3=3
      N7=72
C     PUNCH THICKNESSES
      WRITE (7,1008) N3,T(1,1),T(1,2)
      WRITE (7,1008) N1,T(4,1),T(4,2)
      WRITE (7,1008) N1,T(5,1),T(5,2)
      WRITE (7,1008) N1,T(6,1),T(6,2)
      WRITE (7,1008) N1,T(7,1),T(7,2)
      WRITE (7,1008) N7,T(8,1),T(8,2)
1008 FORMAT (I3,2E12.5)
      N8=79
      WRITE (7,1019) N8,E1,E2,E3,E4,E5
1019 FORMAT (I3,5E12.5)
C     *****
C
C     END OF GEOMETRY AND CONTROL DATA. BEGIN THE LOAD COMPUTATION
C     LOADS WILL BE GENERATED FOR EACH OF 4 HARMONICS: 0,1,2,AND 4.
C     ONLY HARMONIC 0 INVOLVES THE UPWARD ACCELERATION
C
C     THE FOLLOWING VARIABLES WILL BE USED HEREAFTER
C
C     PHI(I,J) = MERIDIONAL SLOPE OF ELEMENT I AT END J
C     T(I,J) = THICKNESS OF ELEMENT I AT END J
C     Z(I,J) = HEIGHT OF ELEMENT I AT END J
C     R(I,J) = RADIUS OF ELEMENT I AT END J
C
C     HARMONIC 0
C
C     *****
      WRITE (7,1003) NZERO,NZERO
      WRITE (6,1009)
C     *****
C
C     GET HORIZONTAL ACCELERATION AND HYDROSTATIC HEAD
C
C     GSIDE = HORIZONTAL ACCELERATION
C     WH = HYDROSTATIC HEAD
C     GUP = VERTICAL ACCELERATION = 2/3*GSIDE
C
C     *****
1009 FORMAT (' GSIDE,WH')
      READ (5,1000) GSIDE,WH
      GUP=.666667*GSIDE
C     *****
C
C     ELEMENTS 1 - 3 CONTAIN THE FOLLOWING CONTRIBUTIONS.

```

```

C
C      (1.0+GUP)*RHOW*(WH-Z) = HYDROSTATIC AND INERTIA LOADS DUE TO
C      WATER
C      (1.0+GUP)*RHOA*T = GRAVITY AND INERTIA LOAD DUE TO WALL
C
C      ****
C      F1=0.0
C      F2=0.0
C      F3=(1.0+GUP)*RHJW*(WH-Z(1,1))+(1.0+GUP)*RHOA*T(1,1)
C      ****
C
C      F4,F5, AND F6 ARE THE SAME AS F1,F2 AND F3
C
C      ****
C      F4=0.0
C      F5=0.0
C      F6=F3
C      WRITE (7,1010) N3,ZERO,ZERO,F3,ZERO,ZERO,F6
1010  FORMAT (I3,6E12.5)
C      ****
C
C      ELEMENTS 4 - 7 CONTAIN CONTRIBUTIONS FROM BOTH HORIZONTAL AND
C      VERTICAL MOTION
C
C      ****
C      DO 105 I=4,7
C      ****
C
C      F1 = AXIAL LOAD AT S = 0
C      (1.0+GUP)*RHOA*COS(PHI) = GRAVITY AND INERTIA LOAD DUE TO
C      ALUMINUM
C
C      ****
C      F1=-(1.0+GUP)*RHOA*T(I,1)*COS(PHI(I,1))
C      F2=0.0
C      F3 = NORMAL LOAD AT S = 0
C      ****
C
C      0.31831*GSIDE*2.0*RHOW*R = 0TH HARMONIC WATER INERTIA LOAD DUE
C      TO HORIZONTAL MOTION
C      (1.0+GUP)*RHOW*(WH-Z) = HYDROSTATIC HEAD AND INERTIA LOAD DUE
C      TO VERTICAL MOTION
C      (1.0+GUP)*RHOA*T*SIN(PHI) = GRAVITY AND INERTIA LOAD ASSOCIATED
C      WITH WALL MATERIAL
C
C      ****
C      F3=0.31831*GSIDE*2.0*RHOW*R(I,1)+(1.0+GUP)*RHOW*(WH-Z(I,1))+
1(I.0+GUP)*RHOA*T(I,1)*SIN(PHI(I,1))
C      ****
C
C      LOADS F4,F5, AND F6 ARE THE SAME AS F1,F2, AND F3 BUT EVALUATED
C      AT S=L
C
C      F4=-(1.0+GUP)*RHOA*T(I,2)*COS(PHI(I,2))
C      F5=0.0
C      F6=0.31831*GSIDE*2.0*RHOW*R(I,2)+(1.0+GUP)*RHOW*(WH-Z(I,2))+
1(1.0+GUP)*RHOA*T(I,2)*SIN(PHI(I,2))
C      WRITE (7,1010) NONE,F1,ZERO,F3,F4,ZERO,F6
105  CONTINUE
C      N2=2
C      LOADS FOR VERTICAL PORTION OF INNER VESSEL
C      DO 881 I=1,72
C      ****
C
C      THICKNESS IS CONSTANT IN THIS PORTION
C      F1 = AXIAL LOAD AT S = 0

```

```

C
C      (1.0+GJP)*RHOA*T = GRAVITY AND INERTIA LOAD DUE TO WALL
C      MATERIAL
C
C      *****
C      F1=-(1.0+GJP)*RHOA*T(9,1)
C      F2=0.0
C      *****
C
C      F3 = NORMAL LOAD AT S = 0
C
C      GSIDE*RHOW*2.0*0.31831*R = 9TH HARMONIC COMPONENT OF WATER
C      LOAD DUE TO HORIZONTAL MOTION
C      (WH-Z)*RHOW = HYDROSTATIC LOAD
C
C      *****
C      F3=GSIDE*RHOW*2.0*0.31831*R(I,1)+(WH-Z(I,1))*RHOW
C      *****
C
C      F4,F5, AND F6 ARE THE SAME FORM AS F1,F2, AND F3 EXCEPT THAT
C      THEY ARE EVALUATED AT S=L
C
C      *****
C      F4=-(1.0+GJP)*RHOA*T(9,2)
C      F5=0.0
C      F6=GSIDE*RHOW*2.0*0.31831*R(I,2)+(WH-Z(I,2))*RHOW
C      WRITE (7,1010) N1,F1,ZERO,F3,F4,ZERO,F6
C
C 881 CONTINUE
C      HARMONIC 1A
C      *****
C
C      LOADS FOR HARMONIC 1 ARE DUE TO WALL INERTIA AND THE 1ST
C      HARMONIC TERM FROM THE FOURIER SERIES FOR THE WATER INERTIA
C      LOADS
C
C      *****
C      WRITE (7,1003) N1,N1
C      *****
C
C      ELEMENTS 1 - 3 INVOLVE ONLY THE WALL LOADS
C
C      F1 = AXIAL LOAD AT S = 0
C
C      GSIDE*RHOA*T = WALL INERTIA LOAD
C
C      F1=GSIDE*RHOA*T(1,1)
C      F2=0.0
C      F3=0.0
C      F4 IS THE SAME AS F1
C      F4=GSIDE*RHOA*T(1,2)
C      F5=0.0
C      F6=0.0
C      WRITE (7,1010) N3,F1,ZERO,ZERO,F4,ZERO,ZERO
C      *****
C
C      ELEMENTS 4 - 72 INCLUDE BOTH WATER AND WALL TERMS
C
C      *****
C      N4=4
C      DO 106 I=4,7
C      *****
C
C      F1 = AXIAL LOAD AT S = 0
C
C      GSIDE*RHOA*T*SIN(PHI) = WALL INERTIA LOAD

```

```

C
C *****
F1=GSIDE*RHOA*T(I,1)*SIN(PHI(I,1))
F2=0.0
C *****
C
C F3 = NORMAL LOAD AT S = 0
C
C GSIDE*RHOA*T*COS(PHI) = WALL INERTIA LOAD
C GSIDE*2.0*RHO*W*R*0.5 = 1ST HARMONIC CONTRIBUTION OF WATER
C INERTIA
C
C *****
F3=GSIDE*RHOA*T(I,1)*COS(PHI(I,1))+GSIDE*2.0*RHO*W*R(I,1)*0.5
C *****
C
C F4,F5, AND F6 ARE THE SAME FORM AS F1,F2, AND F3 BUT EVALUATED AT
C S=L
C
C *****
F5=0.0
F6=GSIDE*RHOA*T(I,2)*COS(PHI(I,2))+GSIDE*2.0*RHO*W*R(I,2)*0.5
WRITE (7,1010) N1,F1,ZERO,F3,F4,ZERO,F6
106 CONTINUE
C *****
C
C FOR ELEMENTS 8 - 72 THE LOADS ARE SAME AS 4 - 7 BUT WITH PHI=0.0
C AND T=CONST. ALSO NOTE THAT F3=F6
C
C *****
F1=0.0
F2=0.0
F3=GSIDE*RHOA*T(8,1)+GSIDE*0.5*2.0*R(8,1)*RHO
F4=0.0
F5=0.0
F6=F3
WRITE (7,1011) N7,ZERO,ZERO,F3,ZERO,ZERO,F6
C *****
C
C FOR HARMONICS 2 AND 4 THE ONLY CONTRIBUTIONS ARE FROM THE WATER
C INERTIA TERMS
C
C *****
C HARMONIC 2A
WRITE (7,1003) N2,N1
WRITE (7,1010) N3,ZERO,ZERO,ZERO,ZERO,ZERO,ZERO
DO 107 I=4,7
F3=0.21221*GSIDE*2.0*R(I,1)*RHO
F6=0.21221*GSIDE*2.0*R(I,2)*RHO
WRITE (7,1010) N1,ZERO,ZERO,F3,ZERO,ZERO,F6
107 CONTINUE
F3=0.21221*GSIDE*2.0*R(8,1)*RHO
WRITE (7,1010) N7,ZERO,ZERO,F3,ZERO,ZERO,F3
C HARMONIC 4A
WRITE (7,1003) N4,N1
WRITE (7,1010) N3,ZERO,ZERO,ZERO,ZERO,ZERO,ZERO
DO 108 I=4,7
F3=-0.04244*GSIDE*2.0*R(I,1)*RHO
F6=-0.04244*GSIDE*2.0*R(I,2)*RHO
WRITE (7,1010) N1,ZERO,ZERO,F3,ZERO,ZERO,F6
108 CONTINUE
F3=-0.04244*GSIDE*2.0*R(8,1)*RHO
WRITE (7,1010) N7,ZERO,ZERO,F3,ZERO,ZERO,F3
C SABOR 5 PORTION
WRITE (6,1011)
1011 FORMAT (' SABOR5 TITLE?')

```

```

READ (5,1005) (TIT(I),I=1,20)
WRITE (7,1005) (TIT(I),I=1,20)
WRITE (7,1003) N1,NZERO,NZERO,N1,NZERO,NZERO,NZERO,N1
WRITE (7,1003) NZERO,NZERO,N2,NZERO
N0=0
N9=89
N33=3
N4=4
WRITE (7,1003) N0,N0,N0,N0,N0,N0,N0,N0,N0
WRITE (7,1003) N2,N4
WRITE (7,1003) N4,N9,N33
WRITE (7,1003) N1,N1,N2,N2
WRITE (7,1003) N0,N0,N0,N0,N0,N0,N0,N0,N0
WRITE (7,1003) N2,N4
WRITE (7,1003) N4,N9,N33

```

C
C
C
C
C
C
C

```

*****
RING LOAD DUE TO TREATMENT OF FUEL ELEMENTS AND ASSOCIATED
STRUCTURE AS LUMPED MASS. COMPUTATION YIELDS FACT THAT THIS
CONTRIBUTION IS INSIGNIFICANT EVEN FOR LARGE GSIDE. SEE NOTES

```

```

*****
F1=300.0/(2.0*3.141593*R(9.1))*GSIDE
F3=300.0/(2.0*3.141593)*GSIDE
WRITE (7,1006) N1,N1,F1
WRITE (7,1006) N1,N4,F3
DO 109 I=2,4,2
WRITE (7,1003) I,N1,N2,N0
WRITE (7,1003) N0,N0,N0,N0,N0,N0,N0,N0,N0
WRITE (7,1003) N2,N4
WRITE (7,1003) N4,N9,N33

```

109 CONTINUE
950 CONTINUE
CALL EXIT
END

Appendix C

Fortran IV Computer Loads Program used to generate loading input to SABOR-5 for the outer core tank.


```

C
C   PROGRAM TO CALCULATE OUTER VESSEL LOADS
C
C   THERE ARE SIX LOADS ASSOCIATED WITH EACH ELEMENT AND THEY ARE
C   DENOTED BY
C       F1,F2,.....,F6 AND THEY REPRESENT
C
C       F1=AXIAL LOAD AT S=0
C       F2=CIRCUMFERENTIAL LOAD AT S=0
C       F3=NORMAL LOAD AT S=0
C       F4=AXIAL LOAD AT S=L
C       F5=CIRCUMFERENTIAL LOAD AT S=L
C       F6=NORMAL LOAD AT S=L
C
C   LOADS FOR TWO HARMONICS FOR EACH OF THE CONDITIONS ARE
C   GENERATED
C
C   *****
C   DIMENSION X(100),PHI(100,2),T(100,2),R(100,2),Y(100),Z(100,2),
C   ITIT(120),NX(4),IHAR(4),FACT(4),A(10)
C   DIMENSION JHAR(4)
C   READ (5,2884) NTIME,{JHAR(I),I=1,4},NTHET,NSTOP
2884  FORMAT (7I4)
C   DENSITY OF WATER IN LBS/(CUBIC IN)
C   RHOW=0.03613
C   DENSITY OF ALUMINUM IN LBS/(CUBIC IN)
C   RHOA=0.1
C   MASS DENSITY OF ALUMINUM
C   XMASS=RHOA/32.2
C   NUMBER OF NODES
C   NODES=95
C   NUMBER OF ELEMENTS
C   NEL=94
C   N3=3
C   MISCELLANEOUS CONSTANTS USED FOR CONTROL OF SABOR5
C   NQ=JHAR(1)+JHAR(2)+JHAR(3)+JHAR(4)
C   FACT(1)=0.5/3.141593
C   FACT(2)=1.0/3.141593
C   FACT(3)=FACT(2)
C   FACT(4)=FACT(3)
C   N1=1
C   IST=0
C   N0=0
C   N4=4
C   N10=10
C   N94=94
C   ZERO=0.0
C   N2=2
C   N4=4
C   N83=83
C   N12=12
C   PHIREF=1.57080
1010  FORMAT (2E12.5)
C   *****
C
C   FROM HERE TO POINT NOTED READ IN GEOMETRY AND MATERIAL PROPERTIES
C
C   *****
C   READ (5,1000) (X(I),Y(I),I=1,NODES)
C   DO 100 I=1,NEL
C   Z(I,1)=X(I)
C   Z(I,2)=X(I+1)
C   R(I,1)=Y(I)

```

```

100 R(I,2)=Y(I+1)
1000 FORMAT (2E12.5)
1005 FORMAT (20A4)
      READ (5,1001) (PHI(I,1),PHI(I,2),I=1,NEL)
      DO 101 I=1,8
      READ (5,1002) N,T1,T2
1002 FORMAT (I3,2E12.6)
1001 FORMAT (8X,2E12.5)
      IBFG=IST+1
      IFND=IST+N
      DO 102 J=IBFG,IFND
      T(J,1)=T1
102 T(J,2)=T2
101 IST=IST+N
      READ (5,1043) E1,E2,E3,E4,E5
1043 FORMAT (3X,5E12.5)
C *****
C
C      END OF GEOMETRY INPUT
C
C      LOOP 950 CONTROLS CALCULATION FOR THE NUMBER OF CASES DESIRED
C      NORMALLY NTIME = 3 FOR THE THREE LOADS GSIDE=0.5,2.5,4.5
C
C      *****
C      WRITE (6,1009)
1009 FORMAT (' GSIDE,WH?')
C *****
C
C      GET HORIZONTAL ACCELERATION AND HYDROSTATIC HEAD
C
C      GSIDE = HORIZONTAL ACCELERATION
C      WH = HYDROSTATIC HEAD
C      GUP = VERTICAL ACCELERATION = 2/3*GSIDE
C
C      *****
C      READ (5,1010) GSIDE,WH
C      PUNCH GEOMETRY AND SABORS CONTROL DATA
C      GUP=.666667*GSIDE
      WRITE (7,1003) NO,NEL,NODES,NO,NQ,NC,NO,N1,N10,NC,N1
1003 FORMAT (11I4)
      WRITE (6,1004)
1004 FORMAT (' LANCES TITLE?')
      READ (5,1005) (TIT(I),I=1,20)
      WRITE (7,1005) (TIT(I),I=1,20)
      WRITE (7,1003) NO
      WRITE (7,1000) (X(I),Y(I),I=1,NODES)
      I=1
      J=2
      WRITE (7,1006) I,J,PHI(I,1),PHI(I,2),N94
1006 FORMAT (2I4,2E12.5,8X,I4)
      DO 103 I=2,83
      J=I+1
      WRITE (7,1006) I,J,PHI(I,1),PHI(I,2)
103 CONTINUE
      K=1
      J=85
      I=84
      WRITE(7,1006) K,J,PHI(I,1),PHI(I,2)
      DO 4147 I=85,94
      J=I+1
      WRITE(7,1006) I,J,PHI(I,1),PHI(I,2)
4147 CONTINUE
      WRITE (7,1007) (N1,T(I,1),T(I,2),XMASS,I=1,NEL)
1007 FORMAT (I3,3E12.5)
      WRITE (7,1008) NEL,E1,E2,E3,E4,E5
1008 FORMAT (I3,6E12.5)

```

```

C      TERMINATE IF ONLY GEOMETRY WANTED
C      IF (NSTOP .NE. 0) CALL EXIT
C      *****
C
C      END OF GEOMETRY AND CONTROL DATA. BEGIN THE LOAD COMPUTATION
C      LOADS WILL BE GENERATED FOR EACH OF 4 HARMONICS: 0,1,2,AND 4.
C      ONLY HARMONIC 0 INVOLVES THE UPWARD ACCELERATION
C
C      THE FOLLOWING VARIABLES WILL BE USED HEREAFTER
C
C      PHI(I,J) = MERIDIONAL SLOPE OF ELEMENT I AT END J
C      T(I,J) = THICKNESS OF ELEMENT I AT END J
C      Z(I,J) = HEIGHT OF ELEMENT I AT END J
C      R(I,J) = RADIUS OF ELEMENT I AT END J
C
C      HARMONIC 0
C
C      *****
C      WRITE (7,1906) NO,NO
C      IF (JHAR(1) .EQ. 0) GO TO 176
C      DO FOR ALL ELEMENTS
C      NET=1
C      NEL=34
C      NIR=-1
8592  CONTINUE
C      DO 104 I=NET,NEL
C      *****
C
C      F1 = AXIAL LOAD AT S = 0
C
C      (1.0+GUP)*RHOA*T* $\cos(\text{PHI})$  = GRAVITY AND INERTIA LOAD ASSOCIATED
C      WITH WALL MATERIAL
C
C      *****
C      F1=-RHOA*(1.0+GUP)*T(I,1)* $\cos(\text{PHI}(I,1))$ 
C      F2=0.0
C      *****
C
C      F3 = NORMAL LOAD AT  $S = 0$  AND IS COMPOSED OF THE FOLLOWING TERMS
C
C      (WH-Z)*RHOW = HYDROSTATIC WATER LOAD
C      (WH-Z)*GUP*RHOW*SIN(PHI) = WATER INERTIA LOAD DUE TO
C      VERTICAL MOTION OF VESSEL
C      (1.0+GUP)*SIN(PHI)*RHOA = INERTIA AND GRAVITY LOAD DUE
C      TO VERTICAL MOTION OF THE WALL
C
C      *****
C      F3=(WH-Z(I,1))*RHOW+(WH-Z(I,1))*GUP*RHOW*SIN(PHI(I,1))+(1.0+GUP)*
C      T(I,1)*SIN(PHI(I,1))*RHOA
C      *****
C
C      THE LOADS F4,F5, AND F6 CONTAIN THE SAME CONTRIBUTIONS AS DO
C      F1,F2, AND F3. BUT ARE EVALUATED AT S=L OF THE ELEMENT
C
C      *****
C      F4=-RHOA*(1.0+GUP)*T(I,2)* $\cos(\text{PHI}(I,2))$ 
C      F5=0.0
C      F6=(WH-Z(I,2))*RHOW+(WH-Z(I,2))*GUP*RHOW*SIN(PHI(I,2))+(1.0+GUP)*
C      T(I,2)*SIN(PHI(I,2))*RHOA
C      WRITE (7,1008) N1,F1,ZERO,F3,F4,ZERO,F6
104  CONTINUE
C      IF(NIR) 8593,8594,8595
8593  NET=35
C      NEL=37
C      NIR=0
C      RHOA=8.6

```

```

      GO TO 8592
8594 NET=38
      NEL=94
C
      NIR=10
      RHOA=0.1
      GO TO 8592
8595 CONTINUE
C
C      IN THE FEET AREA OF THE FEET, THE FEET ARE TREATED AS A DISTRIBUTED LOADIN
C      IN THE FEET AREA OF THE FEET, THE FEET ARE TREATED AS
C      DISTRIBUTED LOADING BY INCREASING THE DENSITY OF THE TANK
C
C      *****
C
C      HARMONIC 1A INVOLVES ONLY SIDEWAYS ACCELERATIONS
C
C      *****
176 IF (JHAR(2) .EQ. 0) GO TO 8599
      WRITE (7,1006) N1,N1
C      FOR ALL ELEMENTS
      NET=1
      NEL=34
      NIR=-1
8596 CONTINUE
      DO 105 I=NET,NEL
C      *****
C      LOADS F2 AND F5 ARE BOTH ZERO. THE GRAVITY LOAD EXISTS ONLY FOR
C      HARMONIC 0. LOADS IN THE AXIAL AND NORMAL DIRECTION DEPEND ONLY
C      ON THE LOCAL MERIDIONAL SLOPE AND ARE DUE ONLY TO THE WALL
C      MATERIAL
C
C      *****
      F1=GSIDE*RHOA*(I,1)*SIN(PHI(I,1))
      F3=GSIDE*RHOA*(I,1)*COS(PHI(I,1))
      F4=GSIDE*RHOA*(I,2)*SIN(PHI(I,2))
      F6=GSIDE*RHOA*(I,2)*COS(PHI(I,2))
      WRITE (7,1008) N1,F1,ZERO,F3,F4,ZERO,F6
105 CONTINUE
      IF (NIR) 8597,8598,8599
8597 NET=35
      NEL=37
      NIR=0
      RHOA=19.1
      GO TO 8596
8598 NET=38
      NEL=94
      RHOA=0.1
      NIR=10
      GO TO 8596
8599 CONTINUE
C      SABOR5
179 WRITE (6,1011)
1011 FORMAT (' SABOR5 TITLE?')
      READ (5,1005) (TIT(I),I=1,20)
      WRITE (7,1005) (TIT(I),I=1,20)
      WRITE (7,1003) N1,N1,ND,N1,ND,ND,ND,N1
      IHAR(1)=0
      IHAR(2)=1
      IHAR(3)=2
      IHAR(4)=4
      NX(1)=3
      NX(2)=1

```

```

NX(3)=1
NX(4)=1
N8=8
DO 106 I=1,4
IF (JHAR(I) .EQ. 0) GO TO 106
NO=0
WRITE (7,1003) IHAR(I),NX(I),N1,NO
WRITE (7,1003) NO,NO,NO,NO,NO,NO,NO,NO
WRITE (7,1003) N1,N83
106 CONTINUE
C *****
C FROM HERE TO END IS CONTROL DATA FOR THE PLOT PROGRAM
C *****
C *****
DO 210 I=1,NTHET
210 A(I)=45.0*(I-1)
WRITE (7,1003) NTHET,NO,NO
WRITE (7,1022) (A(I),I=1,NTHET)
1022 FORMAT (8F10.3)
A(1)=0.0
A(2)=0.5
A(3)=1.0
DO 211 I=1,NTHET
WRITE (7,1003) NO,NO,N3
WRITE (7,1023) (A(J),J=1,3)
1023 FORMAT (3E12.5)
211 CONTINUE
950 CONTINUE
CALL EXIT
END

```

Appendix D

Fortran IV Computer Program used in Determination of
Fundamental Frequency of the Core Tank using the Method of
Vianello and Stodola (H3).

Figure D.1 Assumed Initial Displacements

```

C
PROGRAM TO DETERMINE THE FUNDAMENTAL FREQUENCY OF THE CORE TANK
C
  DIMENSION T(4,4), A(4,4), XX(4,4)
  DIMENSION C(95),F(95,95),AP(95)
  DIMENSION B(4,4), XY(4,4)
  DIMENSION IWORK(95),JWORK(95),XMAS(95,95)
  DIMENSION WAT(95)
  DIMENSION X(95,95), PHI(100)

C
C
C
C   THE MASS MATRIX AND THE STIFFNESS MATRIX ARE OBTAINED FROM
C   THE SABOR 5 PROGRAM AND CORRESPOND TO THE GEOMETRY USED IN
C   STRESS DETERMINATIONS
C   X(I,J) = STIFFNESS MATRIX
C   XMASS(I,J) = MASS MATRIX
C
C   CALLING ON THE STIFFNESS MATRIX FROM SABOR 5
C   CALL READIN
10  FORMAT(5F10.5)
11  FORMAT(6E13.6)
12  FORMAT(15X,28HX-DIRECTION STIFFNESS MATRIX )
C   READING IN THE VALUES OF PHI
  DO 410 I=1,95
  DO 410 J=1,95
  XMAS(I,J)=0.0
410  X(I,J)=0.0
  READ(5,10)(PHI(J),J=1,95)

C
C
C   SABOR 5 DOES NOT STORE THE FULLY POPULATED MATRIX BUT ONLY
C   STORES THE NON-ZERO TERMS
C   THE FOLLOWING STEPS ARE TO TAKE THE DESIRED COEFFICIENTS
C   FROM THE SABOR MATRIX
C
C
C
C
C   THE COORDINATE SYSTEM MUST BE CHANGED FROM THE SABOR SYSTEM TO
C   AN X - Y - Z SYSTEM
C
C   DETERMINING THE STIFFNESS MATRIX
  CALL ERASE (T,16)
  DO 100 I=1,94
  CSI=CCS(PHI(I))
  SNI=SIN(PHI(I))
  J=I+1
  CALL ERASE (A,16)
  CALL ERASE (B,16)
  CSJ=CCS(PHI(J))
  SNJ=SIN(PHI(J))
  T(1,1)=CSI
  T(2,1)=-SNI
  T(1,2)=SNI
  T(2,2)=CSI
  T(3,3)=CSJ
  T(3,4)=SNJ
  T(4,3)=-SNJ
  T(4,4)=CSJ
  CALL TERM (I,1,I,1,B(1,1),A(1,1))
  CALL TERM (I,1,I,3,B(1,2),A(1,2))

```

```

CALL TERM (I,3,I,3,B(2,2),A(2,2))
CALL TERM (J,1,I,1,B(3,1),A(3,1))
CALL TERM (J,1,I,3,B(3,2),A(3,2))
CALL TERM (J,1,J,1,B(3,3),A(3,3))
CALL TERM (J,3,I,1,B(4,1),A(4,1))
CALL TERM (J,3,I,3,B(4,2),A(4,2))
CALL TERM (J,3,J,1,B(4,3),A(4,3))
CALL TERM (J,3,J,3,B(4,4),A(4,4))
DO 400 K=1,4
DO 400 L=1,K
      B(L,K)=B(K,L)
400  A(L,K)=A(K,L)
DO 401 II=1,4
DO 401 JJ=1,II
      SUMB=C.0
      SUMA=C.0
DO 402 KK=1,4
DO 402 LL=1,4
      SUMB=SUMB+T(KK,II)*B(KK,LL)*T(LL,JJ)
402  SUMA=SUMA+T(KK,II)*A(KK,LL)*T(LL,JJ)
      XY(II,JJ)=SUMA
      XY(JJ,II)=SUMA
      XX(II,JJ)=SUMB
401  XX(JJ,II)=SUMB
      IF (I .NE. 1) GO TO 640
      X(1,1)=XX(1,1)
      XMAS(1,1)=XY(1,1)
640  X(I,J)=XX(1,3)
      X(J,I)=XX(3,1)
      X(J,J)=XX(3,3)
      XMAS(I,J)=XY(1,3)
      XMAS(J,I)=XY(3,1)
      XMAS(J,J)=XY(3,3)
100  CCNTIALF
DO 4050 I=1,95
DO 4050 J=92,95
      XMAS(I,J)=0.0
      XMAS(J,I)=0.0
      X(I,J)=0.0
4050  X(J,I)=0.0
DO 4051 J=92,95
      XMAS(J,J)=1.0
4051  X(J,J)=1.0
DO 1001 I=1,95,10
      IST=I
      IED=MIN0(I+9,95)
3345  FORMAT(1X,10E12.4)
      WRITE (6,3345) ((X(K,J),J=IST,IED),K=1,95)
1001  CONTINUE
C
C
C      INVERTING THE STIFFNESS MATRIX YIELDS THE FLEXIBILITY MATRIX
C
      ABG=0.0
DO 800 I=1,95
800  ABG=ABG+ALOG(X(I,I))
      ABG=ABG/95.0
      ABG=EXP(ABG)
      ABG=1.0/ABG
DO 801 I=1,95
DO 801 J=1,95
801  X(I,J)=X(I,J)*ABG
      CALL MINV (X,95,D,IWORK,JWORK)
DO 802 I=1,95
DO 802 J=1,95
802  X(I,J)=X(I,J)*ABG

```



```

2245 FORMAT (I4)
2246 FORMAT (5E12.6)
      READ(5,2245) JOT
2247 FORMAT (5X,I4,5X,36HFUNDCAMENTAL FREQUENCY OF CORE TANK )
      WRITE(6,2247) JOT
C
C
C   AN INITIAL SET OF DISPLACEMENTS IS ASSUMED
C
C   READING IN THE ASSUMED DISPLACEMENTS
C
C   THE MASS MATRIX FROM THE SABOR PROGRAM ONLY INCLUDED THE
C   MASS OF THE TANK, THUS THIS MASS MUST BE INCREASED FOR THE
C   MASS OF THE WATER BY INCLUDING LUMPED MASSES AT EACH NODE
C
C   THE FACTOR OF 32.2 OCCURS BECAUSE SABOR 5 GIVES THE MASS MATRIX
C   IN SLUGS
C
      READ(5,2246) (C(I),I=1,95)
      Z=14.0
      DO 1000 J=19,40
        WAT(J)=0.833*0.833*0.0833*3.14*62.4/32.2
        XMAS(J,J)=XMAS(J,J)+WAT(J)/2.0
1000   XMAS(J+1,J+1)=XMAS(J+1,J+1)+WAT(J)/2.0
        DO 1100 J=41,46
          WAT(J)=0.833*0.833*3.14*0.0333*62.4/32.2
          XMAS(J,J)=XMAS(J,J)+WAT(J)/2.0
1100   XMAS(J+1,J+1)=XMAS(J+1,J+1)+WAT(J)/2.0
        DO 1002 J=47,60
          WAT(J)=(0.833+1.0/Z)**2.0*C.062*3.14*62.4/32.2
          Z=Z-1.0
          XMAS(J,J)=XMAS(J,J)+WAT(J)/2.0
1002   XMAS(J+1,J+1)=XMAS(J+1,J+1)+WAT(J)/2.0
        DO 1003 J=61,65
          WAT(J)=1.87*1.87*0.145*3.14*62.4/32.2
          XMAS(J,J)=XMAS(J,J)+WAT(J)/2.0
1003   XMAS(J+1,J+1)=XMAS(J+1,J+1)+WAT(J)/2.0
          XMAS(66,66)=XMAS(66,66)+(1.87*1.87*0.30*3.14*62.4/64.4)
          XMAS(67,67)=XMAS(67,67)+(1.87*1.87*0.30*3.14*62.4/64.4)
        DO 1004 J=67,71
          WAT(J)=1.87*1.87*3.14*C.162*62.4/32.2
          XMAS(J,J)=XMAS(J,J)+WAT(J)/2.0
1004   XMAS(J+1,J+1)=XMAS(J+1,J+1)+WAT(J)/2.0
        DO 1005 J=72,92
          WAT(J)=2.083*2.083*0.145*3.14*62.4/32.2
          XMAS(J,J)=XMAS(J,J)+WAT(J)/2.0
1005   XMAS(J+1,J+1)=XMAS(J+1,J+1)+WAT(J)/2.0
        DO 1006 J=93,94
          WAT(J)=2.083*2.083*3.14*C.33*62.4/32.2
          XMAS(J,J)=XMAS(J,J)+WAT(J)/2.0
1006   XMAS(J+1,J+1)=XMAS(J+1,J+1)+WAT(J)/2.0
          XMAS(48,48)=XMAS(48,48)+750.0/32.2
          XMAS(49,49)=XMAS(49,49)+750.0/32.2
          XMAS(50,50)=XMAS(50,50)+750.0/32.2
C
C
C   THE MASS MATRIX AND THE FLEXIBILITY MATRIX ARE MULTIPLIED
C   TOGETHER WITH THE ASSUMED DISPLACEMENTS TO GIVE A LAMBDA AND A
C   NEW SET OF DISPLACEMENTS
C
      CALL ERASE (AP,95)
      CALL ERASE (F,9025)
      DO 101 I=1,95

```

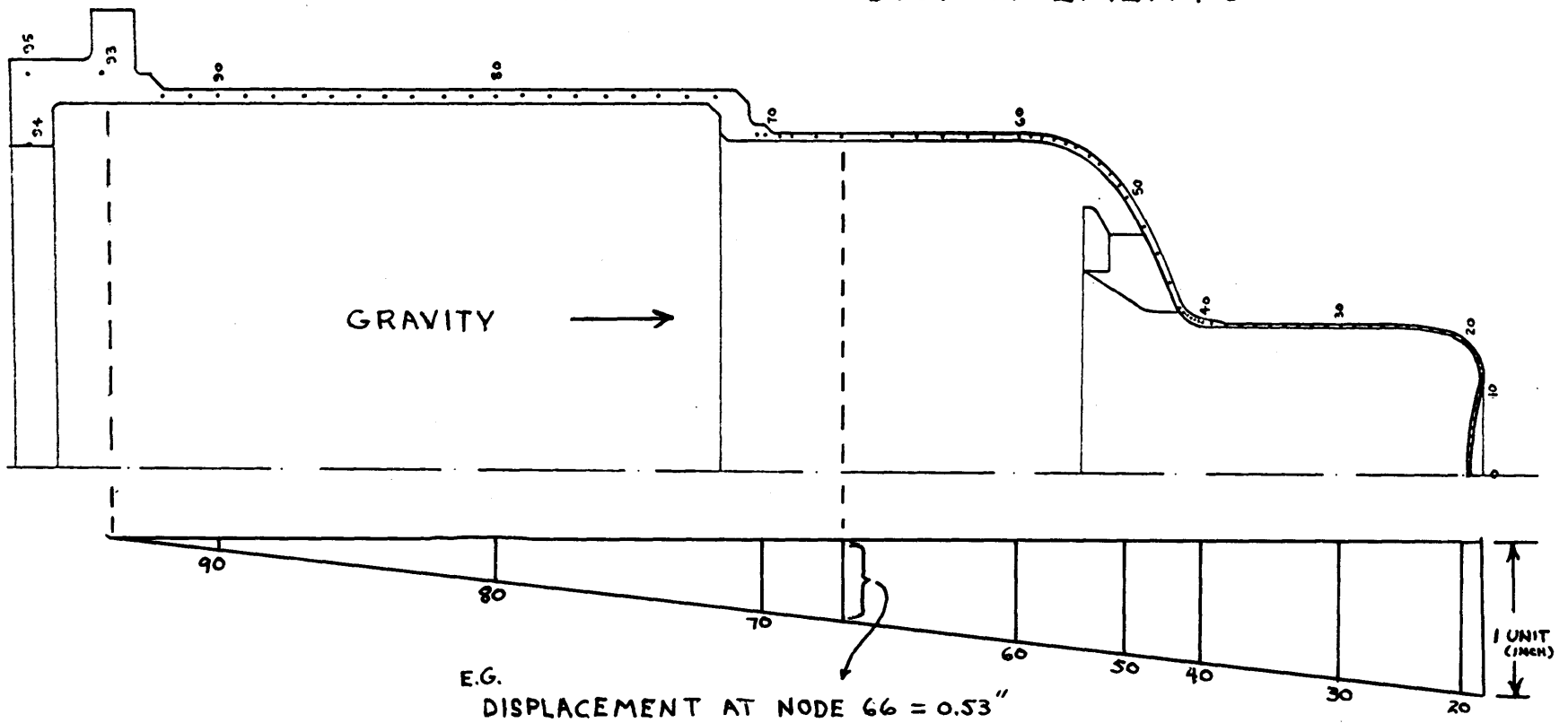
```

      DO 101 J=1,I
      SUM=0.0
      DO 750 K=1,95
750    SUM=SUM+32.2*X(I,K)*XMAS(K,J)
      F(I,J)=SUM
101    F(J,I)=SUM
2248  FORMAT(2X,10HLAMBDA = ,E12.6)
1050  FORMAT(5X,4HNODE,10X,11HLUMPED MASS,10X,15HX-DISPLACEMENT )
1051  FORMAT(5X,I4,9X,E12.6,12X,E12.6)
      L=100
      II=0
200   C=C.0
      DO 102 J=1,95
      DO 2005 I=1,95
      AP(J)=AP(J)+(F(J,I)*D(I))
2005  CONTINUE
      IF(AP(J)-C) 201,201,202
202   C=AP(J)
201   CONTINUE
102   CONTINUE
      II=II+1
901   DO 300 J=1,95
      D(J)=AP(J)/C
C
C   THE PROCESS IS ITERATES 100 TIMES
C   C = LAMBDA
C   R = CMEGAC
C
300   CONTINUE
      WRITE (6,2248) C
      IF(L-II) 900,900,200
900   R=SQRT(1.0/C)
950   FORMAT(2X,30CMEGA FOR THE MITR-2 VESSEL IS,2X,E12.6)
      WRITE(6,950) R
      WRITE(6,1050)
      DO 1009 J=1,95
      WRITE(6,1051) J,XMAS(J,J),C(J)
1009  CONTINUE
      CALL EXIT
      END
      SUBROUTINE READIN
      DIMENSION XK(2454),XM(2454),NCOL(400)
C
C   SUBROUTINE READIN OBTAINS THE THE STIFFNESS AND MASS
C   MATRICES FROM THE STORAGE LOCATION OF THE SAVOR 5
C   PROGRAM USED IN RUNNING THE STRESS ANALYSIS
C
C
      INTEGER*4 D1,D2
      DO 100 I=5,380,4
      J=I-4
      NCCL(I)=J
      NCCL(I+1)=J
      NCCL(I+2)=J
      NCCL(I+3)=J
      WRITE (6,4000) I,NCOL(I),NCOL(I+1),NCOL(I+2),NCOL(I+3)
4000  FORMAT (5I10)
      100 CONTINUE
      DO 101 I=1,4
      NCCL(I)=1
      READ (8,1000) (XM(I),I=1,2454)
1000  FORMAT (6F12.6)
      READ (8,1000) (XK(I),I=1,2454)
      RETURN
      ENTRY TERM (N1,D1,N2,D2,VALUE1,VALUE2)
      IRCW1=(N1-1)*4+D1

```

```
IRCW2=(N2-1)*4+D2
IRCW=MAXO(IRCW1,IRCW2)
ICCL=MINO(IRCW1,IROW2)
INDEX=ICOL
IF (ICOL .GE. NCOL(IROW) .AND. ICOL .LE. IROW) GO TO 103
WRITE (6,1001) N1,D1,N2,D2
1001 FORMAT (/ ' THE VALUES N1,D1,N2,D2 = ',3(I4,', '),I4,' FORM AN INVAL
LID COMBINATICN. VALUE1 AND VALUE2 ARE SET TO 0.0')
VALUE1=0.0
VALUE2=0.0
RETURN
103 DO 102 I=1,IRCW
102 INDEX=INDEX+I-NCOL(I)
VALUE1=XK(INDEX)
VALUE2=XM(INDEX)
RETURN
END
```

FIGURE D.1
 ASSUMED INITIAL DISPLACEMENTS



Appendix E

CALCULATION OF FUNDAMENTAL MODE OF COOLANT PIPE

The main light water coolant pipe is the longest unrestrained major pipe. The pipe will be constrained against large motions because of the tightness of the area through which it passes.

The dimensions of the pipe are:

$$D_o = \text{outside diameter} = 8.5 \text{ inches}$$

$$D_i = \text{inside diameter} = 8.0 \text{ inches}$$

$$l = \text{length} = 15 \text{ feet}$$

$$I = \text{Moment of inertia} = \frac{\pi(D_o^4 - D_i^4)}{64} = 56 \text{ inches}^4$$

$$E = \text{modulus of elasticity of aluminum} = 0.1 \times 10^8 \text{ pounds/inches}^2$$

the mass of the pipe and water is:

$$m = \pi((D_o/2)^2 - (D_i/2)^2) (l) (\rho_{Al}) + \pi(D_i/2)^2 l (\rho_{H_2O}) \quad (E.1)$$

$$\text{where } \rho_{Al} = \text{density of aluminum} = 0.1 \text{ pounds/inch}^3$$

$$\rho_{H_2O} = \text{density of water} = 0.036 \text{ pounds/inch}^3$$

thus

$$m = 442 \text{ pounds}$$

Now assuming the coolant pipe acts as a circular pipe with fixed ends, the fundamental mode is:

$$w = \frac{25 \pi^2}{16 l} \sqrt{\frac{E I}{m}} \quad (E.2)$$

thus

$$\begin{aligned} w &= \frac{25 (3.14)^2}{16 (12 \times 15)} \sqrt{\frac{(0.1 \times 10^8) (56)}{(442)}} & (E.3) \\ &= 97 \text{ cycles/sec.} \end{aligned}$$

Appendix F

CALCULATION OF GUIDE TUBE DISPLACEMENT
FROM 1 G HORIZONTAL ACCELERATION

Referring to Figure 3.5, the displacement of a control guide tube of length ℓ is to be determined at distance X from where ℓ equals 0. The guide tube is modeled as a cantilever beam which is fixed at $\ell = 0$.

For a cantilever beam under a distributed loading, the displacement at X is : (M1)

$$X = \frac{w}{24 EI} (\ell^4 - 4\ell^3 X + 3\ell^2 X^2) \quad (F.1)$$

For a cantilever beam with a concentrated load at ℓ , the displacement at X is: (M1)

$$X = \frac{P}{6 EI} (2\ell^3 - 3\ell^2 X + X^3) \quad (F.2)$$

where

E = modulus of elasticity

I = moment of inertia of the guide tube

P = concentrated load at length = ℓ

w = distributed load (pounds/inch)

The mass of the guide tube acts as a distributed load during a horizontal acceleration, and the mass of the guide rod and blade is assumed to act as a concentrated load at ℓ during a horizontal acceleration. For a 1 G acceleration, the loads equal the respective gravitational mass of the guide tube and rod.

Now

$$X = 31 \text{ inches}$$

$$l = 48 \text{ inches}$$

$$E = .1 \times 10^8 \text{ pounds/inches}^2$$

$$D_o = \text{outside diameter of guide tube} = 3 \text{ inches}$$

$$D_i = \text{inside diameter of guide tube} = 2 \text{ inches}$$

$$I = \frac{\pi (D_o^4 - D_i^4)}{64} = 3.2 \text{ inches}^4$$

for a 1 G lateral force

$$P = 25 \text{ pounds}$$

$$w = 0.4 \text{ pounds/inch}$$

(structure is made of aluminum)

The total displacement is the sum of the displacement from the distributed load and the displacement from the concentrated load.

$$\Delta X_{\text{total}} = \frac{w}{24 EI} (X^4 - 4l^3 X + 3l^4) \quad (\text{F.3})$$

$$+ \frac{P}{6 EI} (2l^3 - 3l^2 X + X^3)$$

$$X = \frac{0.4}{(24)(1 \times 10^7)(3.2)} ((31)^4 - 4(48)^3(31) + 3(48)^4)$$

(F.4)

$$+ \frac{25}{6(1 \times 10^7)(3.2)} (2(48)^3 - 3(48)^2(31) + (31)^3)$$

thus

$$X = 0.00634 \text{ inches}$$

Appendix G
FORTRAN IV COMPUTER PROGRAM USED FOR
APPROXIMATE STACK ANALYSIS

Dimensions of Stack

Height = 150 feet

Outside Radius at the bottom of the stack = 7.21 feet

Inside Radius at the bottom of the stack = 5.83 feet

Outside Radius at the top of the stack = 1.85 feet

Inside Radius at the top of the stack = 1.25 feet

```

C
C *****
C
C PROGRAM TO CALCULATE THE SHEARING STRESSES ON THE STACK
C THE LOADING IS A COMBINATION OF A 100 MPH WIND
C AND THE SHEAR USING THE SEACO DESIGN CODE
C
C *****
C DIMENSION AH(26),ROH(26),PMASS(25),PMDM(25),FW(25),T(6),V(6)
C DIMENSION SHEAR(6,25)
932 FORMAT(/2X,'OMEGA=((.597*3.1416)/L**12.0)*SQRT(E*I/M)',/2X,
1 'SHEAR=1.5*K*C*W',/2X,'WHERE 1.5 IS A FACTOR INCREASING',
2 'SHEAR FOR CIRCULAR CROSS SECTION',/10X,'K=1.5 FOR BRITTLE',
3 'STRUCTURE',/10X,'W= WEIGHT OF STACK')
933 FORMAT(/10X,'C=0.05/(PERIOD**0.333)',/2X,'A 100 MPH WIND ',
1 'LOAD IS ALSO INCLUDED')
C
C ROBOT = RADIUS AT THE BOTTOM OF THE STACK OUTSIDE
C ROTOP = RADIUS AT THE TOP OF THE STACK OUTSIDE
C RIBOT = RADIUS AT THE BOTTOM OF THE STACK INSIDE
C RITOP = RADIUS AT TOP OF THE STACK INSIDE
C
C RITOP=2.5/2.0
C ROTOP=3.69/2.0
C RIBOT=11.67/2.0
C ROBOT=14.42/2.0
C
X
C THE STACK IS ASSUMED TO BE BRITTLE
C SHEAR = 1.5*K*C*W
C SEACO DESIGN CODE GIVES
C
C
C THE STACK IS DIVIDED INTO 25 SECTIONS AND THE MASS OF EACH
C SECTION IS DETERMINED
C THE MOMENT OF EACH SECTION ABOUT THE BASE IS DETERMINED
C
C ATOP=3.1416*(1.85**2.0-1.25**2.0)
C ABOT=3.1416*(7.21**2.0-5.835**2.0)
C ATAV=(ATOP+ABOT)/2.0
C TMASS=ATAV*150.0*125.0+400.0
C AH(1)=ATOP
C H=0.0
C L=1
C DO 1000 I=2,26
C HH=H+3.0
C HB=H+6.0
C RIH=RITOP+((RIBOT-RITOP)*HB/150.0)
C ROH(I)=ROTOP+((ROBOT-ROTOP)*HB/150.0)
C AH(I)=3.1416*(ROH(I)**2.0-RIH**2.0)
C AAVE=(AH(L)+AH(I))/2.0
C PMASS(L)=AAVE*6.0*125.0
C PMDM(L)=PMASS(L)*(150.0-HH)
C H=H+6.0
C L=L+1
C IF(I-13) 1000,900,1000
900 RIP=RIH*12.0
ROP=ROH(I)*12.0
1000 CONTINUE
E=2000000.0
C
C THE APPROXIMATE MOMENT OF INERTIA IS CALCULATED
C

```

```

MOMI=(3.1416*((2.0*ROP)**4.0-(2.0*RIP)**4.0))/64.0
ML=TMASS/(150.0*144.0)
XL=(150.0*12.0)**2.0
OMEGA=((0.597*3.1416)**2.0/XL)*SQRT(E*MOMI/ML)
TAPP=1.0/OMEGA
PMASS(1)=PMASS(1)+400.0
PMOM(1)=PMOM(1)+(400.0*149.0)
1001 FORMAT(3X,'STACK SHEAR USING THE SEACD DESIGN CODE')
1002 FORMAT(/5X,'TOTAL STACK MASS = ',F10.2)
1005 FORMAT(/3X,'FIRST OMEGA = ',F10.5,4X,'PERIOD = ',F10.5,2X,'SEC')
1003 FORMAT(/2X,'SECTION',3X,'CL HEIGHT',5X,'MASS',8X,'MOMENT',9X,
1 'BOTTOM AREA')
WRITE(6,1001)
WRITE(6,932)
WRITE(6,933)
WRITE(6,1002) TMASS
WRITE(6,1005) OMEGA,TAPP
WRITE(6,1003)
H=147.0
DO 100 J=1.25
L=J+1
1004 FORMAT(4X,I4.6X,F7.2,2X,F12.2,2X,F12.2,2X,F5.1)
WRITE(6,1004) J,H,PMASS(J),PMOM(J),AH(L)
H=H-6.0
100 CONTINUE
TOTM=0.0
DO 200 L=1.25
200 TOTM=TOTM+PMOM(L)
C
C THE WIND LOADING IS APPLIED
C
ROH(1)=ROTOP
DO 300 I=1.25
L=I+1
FW(I)=((ROH(I)+ROH(L))*6.0*22.0)
300 CONTINUE
A=1.0
DO 400 I=1.6
T(I)=TAPP/A
C
C THE SEACD DESIGN CODE IS APPLIED TO OBTAIN THE SHEAR AT EACH
C SECTION
C
V(I)=1.5*TMASS*0.05/(T(I)**0.333)
A=A+1.0
400 CONTINUE
C
C THE SHEARS ARE SUMMED AND PRINTED OUT
DO 5000 J=1.6
SUMA=0.0
SUMB=0.0
C
DO 5000 I=1.25
L=I+1
SUMB=SUMB+PMOM(I)
R=SUMB/TOTM
SUMA=SUMA+FW(I)
SHEAR(J,I)=((R*V(J)+SUMA)/(AH(L)*144.0))*1.5
5000 CONTINUE
8000 FORMAT(/2X,'SECTION',5X,'WIND SHEAR',5X,'TOTAL SHEAR IN PSI')
8001 FORMAT(/2X,'DYNAMIC SHEAR AT BASE =',F10.2,3X,'PERIOD=',F7.2,
1 'SECONDS')
8002 FORMAT(5X,I4.5X,F10.2,5X,F10.2)
C
C
C THE PROGRAM DETERMINES THE SHEARS FOR HIGHER FREQUENCIES AS

```

```
C      WELL TO BE CONSERVATIVE
C
      DO 700 J=1,6
      WRITE(6,8001) V(J),T(J)
      WRITE(6,8000)
      DO 700 I=1,25
      WRITE(6,8002) I,FW(I),SHEAR(J,I)
700   CONTINUE
      CALL EXIT
      END
C
C
```

Appendix H

REFERENCES

- A1. Aldrich, Harl P., Settlement Analysis of the M.I.T. Nuclear Reactor, Cambridge, Massachusetts, August, 1956.
- B1. J.M. Biggs, Introduction to Structural Dynamics, McGraw Hill, New York, 1964.
- B2. Bisplinghoff, Raymond L., Statics of Deformable Solids, Addison-Wesley, Reading, Massachusetts, 1965.
- B3. Buchert, Kenneth P., Buckling of Doubly Curved Orthotropic Shells, University of Missouri, Columbia, Missouri, November, 1965.
- C1. Crandall, Stephen H., An Introduction Into the Mechanics of Solids, McGraw-Hill Co., New York, 1959.
- F1. Freeman, John R., Earthquake Damage and Earthquake Insurance, 1932.
- F2. Fruchbaum, J., Reactor Building Plans and Details, ACF Industries, Buffalo, New York, 1956.
- G1. Gibson, J.E., The Design of Shell Roofs, E. & F. N. Spon Ltd., London, 1968.
- H1. Hansen, R.J., Seismic Design For Nuclear Power Plants, M.I.T. Press, 1970.
- H2. Heck, W.H., Earthquake History of the United States, U.S. Department of Commerce, Serial No. 609, 1938.
- H3. Hildebrand, F.B., Methods of Applied Mathematics, Prentice-Hall, Inc., Englewood Cliffs, New Jersey, 1965.
- H4. Kenichi, Kuwano, "Study on the Seismic Responses of Cylindrical Stacks", Mitsubishi Technical Bulletin, Mitsubishi Heavy Industries, Tokyo, Japan, May, 1966.
- K1. Kotanchik, J.J., Discrete-Element Static Analysis of Bonded, Double-Layer, Thin Shells of Revolution - Part I: Analysis and Evaluation, ASRL TR-139-6, Part I, May, 1968.

- K2. Kotanchik, J.J., Discrete-Element Static Analysis of Bonded, Double-Layer, Thin Shells of Revolution-Part II: The SABOR-5 Program, ASRL TR-139-6, Part II, May, 1969.
- M1. Manual of Steel Construction, American Institute of Steel Construction, Inc., New York, 1967.
- M2. McGannon, H.E., The Making, Shaping and Treating of Steel, United States Steel Corp., 1964.
- M3. Molitor, D.A., Chimneys, Peters Co., Detroit, Michigan, 1938.
- M4. Munkres, J.R., Elementary Linear Algebra, Addison-Wesley Co., Reading, Massachusetts, 1964.
- N1. Nuclear Reactors and Earthquakes, United States Atomic Energy Commission, Washington, D. C., TID-7024, August, 1963.
- O1. O'Connor, James J., Standard Handbook Of Lubrication Engineering, McGraw-Hill Company, New York, 1968.
- S1. Safety Analysis Report for the MIT Research Reactor (MITR-II), M.I.T. Department of Nuclear Engineering, MITNE-115, Sept., 1970.
- W1. Witmer, E., The Transient Linear Elastic Response Analysis of Complex Thin Shells of Revolution Subjected to Arbitrary External Loadings, By the Finite Element Program SABOR-5 Drastic, ASRL TR-146-10, April, 1970.